Suspended sediment concentrations in Alpine rivers: from annual regimes to sub-daily extreme events

Amber van Hamel[1, 2, 3], Peter Molnar[4], Joren Janzing[1, 2, 3], and Manuela Irene Brunner[1, 2, 3]

[1]WSL Institute for Snow and Avalanche Research SLF, Davos Dorf, Switzerland
[2]Institute for Atmospheric and Climate Science, ETH Zurich, Zurich, Switzerland
[3]Climate Change, Extremes and Natural Hazards in Alpine Regions Research Center CERC, Davos Dorf, Switzerland
[4]Institute of Environmental Engineering, ETH Zurich, Zurich, Switzerland

Correspondence: Amber van Hamel (amber.vanhamel@slf.ch)

Abstract. The occurrence of extreme suspended sediment concentrations (SSC) in rivers can have negative impacts on human infrastructure, water quality, and the health of aquatic ecosystems. However, most existing studies have focused on the SSC dynamics of individual catchments or single events. Consequently, large-scale patterns of suspended sediment dynamics remain poorly understood. The objective of this study is to identify spatial differences in (1) the seasonality of SSC and (2) the occurrence of SSC extremes in the Alps. For our analyses, we use 10 years of observed sub-daily SSC data from 38 gauging stations in Switzerland and Austria.

We show that the presence of glaciers, catchment elevation and the onset of the melt season are important drivers of SSC seasonality. However, slightly different processes are important at the event scale, where rainfall is the main driver of SSC extremes, responsible for 85 % of all events. The remaining events are entirely or partly associated with snow and glacial melt, which can account for up to 35 % of the events in high-elevation and partially glaciated catchments. This underscores the disproportionate influence of meltwater on sediment concentrations in high altitude Alpine rivers, which can be explained by the significant contribution of meltwater to overland flow and river discharge in combination with the high sediment availability in glacier forefields. A significant proportion of the extreme events (24 %) resulted in peak SSC values greater than 5 g L^{-1}, highlighting their potential to cause significant harm to aquatic species and river ecosystems.

1 Introduction

The total sediment transported by rivers generally consists of suspended sediment and bedload. The fraction of suspended sediment in the total sediment load can vary greatly as a function of sediment supply, lithology, and catchment size, but on an annual timescale the flux of fine sediment in suspension is often the dominant sediment transport process (Turowski et al., 2010). This study focuses on the suspended sediment concentration (SSC) of rivers in the European Alps. Although suspended sediment is a natural component of rivers, extreme concentrations can have significant impacts on hydropower generation and reservoir sedimentation (Panagos et al., 2024), flood impacts (Nones and Guo, 2023; Vázquez-Tarrío et al., 2024), and water quality (Coffey et al., 2019), including the costs of water treatment and the transport of nutrients and contaminants (Brighenti et al., 2019; Steingruber et al., 2021; Zaharescu et al., 2016). In addition, extreme concentrations can have adverse effects on

riverine ecosystems and aquatic species as they reduce water quality, cause a decline in transparency and sunlight penetration,
and result in the clogging of the gills of fish and other aquatic organisms, which can ultimately have lethal impacts (Bilotta
et al., 2012; Kemp et al., 2011; Newcombe and Macdonald, 1991). Given that the majority of suspended sediment is transported
during a few extreme events (Blöthe and Hoffmann, 2022; Schmidt et al., 2022), it is essential to gain a deeper understanding
of the spatial and temporal dynamics of suspended sediment concentration and its extreme conditions.

In mountain environments, there are three hydro-climatic processes that are the most important for sediment transport to
the river, namely, erosive rainfall, snowmelt and glacial melt (Costa et al., 2018a). Together, these processes are responsible
for the detachment and erosion along hillslopes and for connecting the sediments to the river network by overland flow.
They can also trigger mass wasting events such as debris flows and landslides, which can mobilise even greater amounts of
sediment and potentially lead to very high concentrations of suspended sediment in the river (Battista et al., 2022). In addition,
the combination of rainfall, snow- and glacial melt, and groundwater inflow, controls river discharge, which determines a
river's transport capacity. High flows keep sediment in suspension, allowing it to be transported downstream, and can lead to
additional sediment inputs through channel and bank erosion (Park and Hunt, 2017) and the re-suspension of particles that
have been stored in the river bed (Deng et al., 2024).

Climate plays an important role in controlling sediment erosion and the main transport processes in rivers. Changes in
rainfall, meltwater, snow cover, permafrost and glacier retreat will likely have an impact on erosion along hillslopes, sediment
availability, sediment connectivity with the stream, and the amount of energy available for sediment transport (Hirschberg et al.,
2021; Costa et al., 2018b; Mishra et al., 2020; Mancini et al., 2024). To assess future changes in SSC, a better understanding
of the relationship between these climatic processes and the SSC is needed. This requires a comprehensive understanding of
the current spatial and temporal variations in the general SSC behaviour, as well as the specific characteristics of extreme SSC
events. Nevertheless, there is still limited quantitative understanding of sediment transport in alpine rivers, largely due to the
complex, non-linear and highly stochastic nature of suspended sediment transport. This complexity is a consequence of the
many potential hydro-climatic drivers of sediment transport and their interplay, the numerous processes that regulate sediment
production and availability, and the continuous changes in sediment connectivity.

To date, large-scale, multi-catchment analyses investigating the seasonal and sub-daily dynamics of SSC are scarce. A
considerable number of studies have attempted to predict the seasonal dynamics of sediment transport in different catchments
based on catchment characteristics and hydro-climatic factors (Doomen et al., 2008; Mano et al., 2009; Schmidt et al., 2022;
Costa et al., 2017; Sutari et al., 2020). However, these studies have primarily focused on individual catchments or specific
events, limiting generalizability and our understanding of these processes at larger scales. Those studies that did compare
sediment transport across different catchments, either relied on data sets with limited temporal resolution, i.e. monthly and
annual observations (Hinderer et al., 2013; Li et al., 2020), or focused only on sediment yield without considering sediment
concentration (Haddadchi and Hicks, 2020). In order to gain insights into the relative severity and impact of suspended sediment
events, it is necessary to consider both the suspended sediment yield (SSY) and the SSC. The former describes the actual
amount of sediments that is transported by the river, affects river morphology, and is an indicator of soil loss through water

erosion. The latter is a measure of turbidity and activation of sediment sources and therefore affects water quality and river ecology.

60   Event-scale studies have also received considerable attention in the literature, and the majority of these studies make use of sediment-discharge relationships and hysteresis loops to estimate sediment sources, suspended sediment delivery mechanisms, and landscape connectivity. Although these methods are widely used, they are known to have several limitations. The SSC-discharge relationship (also called the sediment rating curve) is purely empirical and is not able to account for (seasonal) variations in sediment availability (e.g. stocking, depletion and activation of different sediment sources) (Doomen et al., 2008;

65   Horowitz, 2003; Zhang et al., 2021; Costa et al., 2018b). Most studies still use baseflow separation techniques to extract SSC events (Shin et al., 2023; Haddadchi and Hicks, 2021; Blöthe and Hoffmann, 2022; Skålevåg et al., 2024), approaches that often neglect events with high SSC but low discharge. This is a problem from a water quality perspective, because such events are similarly relevant as events associated with high discharge. Furthermore, the use of sediment-discharge hysteresis loops, which describe the relationship between discharge and SSC during an event, has been popular for classifying events

70   and estimating sediment sources (Walling, 1977; Millares and Moñino, 2020). Although the hysteresis method is commonly applied, its results are highly location dependent and the interpretation of hysteresis patterns is challenging due to the influence of feedback mechanisms, interactions between multiple drivers, and the uncertainty regarding the location of sediment sources within the catchment (Skålevåg et al., 2024; Misset et al., 2019). Based on an event classification by Skålevåg et al. (2024), hysteresis explains only about one tenth of the variability of sediment-discharge events. The above limitations call for a novel

75   approach for event classification that does not rely on rating curves and hysteresis patterns. Furthermore, there is a clear need for a more comprehensive understanding of annual and sub-daily patterns in SSC, as well as the occurrence of SSC extremes, across a large domain. Such large-sample analyses could improve our understanding of sediment dynamics not just at the local scale but enable generalizations across multiple catchments.

    To address these research gaps, this study aims (i) to quantify spatial and seasonal differences in the annual SSC regime

80   among catchments and explain these patterns based on catchment characteristics, (ii) to design a classification scheme to distinguish between different extreme SSC event types, and (iii) to explain the spatial and seasonal differences between extreme SSC event types based on event characteristics, seasonally varying characteristics, and antecedent conditions. In this study, we assume that seasonally varying hydro-climatic processes and catchment characteristics, such as changes in precipitation, snow cover and soil moisture, are responsible for the local variation and the inter-event variability of SSC, while characteristics

85   such as geology, altitude and mean annual temperature may be important in explaining the spatial variation in SSC dynamics between catchments.

    The novelty of this study is fourfold: (1) We examine key indicators of the annual SSC regime and extreme SSC events over a large region; (2) We include hydro-climatic forcing (precipitation, snowmelt and glacial melt) prominently in our analyses, event selection, and event classification, as an alternative to the more traditional discharge-based approach; (3) We link annual

90   patterns to sub-daily extremes; and (4) we introduce an event classification scheme that is independent of the SSC-discharge relationship and can be applied to any type of catchment, making it applicable to other regions.

2 Methodology

2.1 Data sets

2.1.1 Suspended sediment concentration (SSC) data

95 For this study, we used data from 38 catchments in the Swiss and Austrian Alps for which turbidity-based suspended sediment concentration data (SSC) were available. These catchments cover different elevations and sizes, with the mean catchment elevation varying from 321 to 2858 m.a.s.l. and catchment areas varying between 22 to 6297 km^2.

For the Austrian stations, we made use of quality-checked 15-minute SSC data for the period 2009–2021 provided by the Austrian Hydrographic Service (Habersack et al., 2017). These data were created by merging manually conducted bi-
100 weekly SSC samples with 15-minute turbidity measurements that are automatically obtained by optical infrared turbidity sensors (Solitax sensors by Hach, concentrations in mg L^{-1}). Combining SSC samples with turbidity data to obtain a high-frequency SSC data set is a commonly applied and accepted method, because of the strong relationship between turbidity and SSC (Gippel, 1995; Grayson et al., 1996). For more details on the methods used by the Austrian Hydrographic Service, see Habersack et al. (2017).

105 For the Swiss stations, bi-weekly SSC samples and 10-minute turbidity data were provided by the Federal Office for the Environment (FOEN) for the period 2014–2023. Unlike the Austrian data, the data had not been quality checked and we had to derive the turbidity-based SSC data ourselves. Due to the gradual replacement of older sensors (which were incapable of correctly detecting high turbidity levels >1000 nephelometric turbidity units (NTU)) with newer and more accurate sensors, the data cleaning resulted in the removal of turbidity levels above 1000 NTU for the period before 2019. Additionally, implausible
110 outliers were removed when the SSC samples were more than 100 times larger than the turbidity-derived values, or vice versa, which resulted in the removal of, on average, three to four values per station. Two additional implausible outliers were removed at the stations of Porte du Scex (Rhône, id 2009) and Bellinzona (Ticino, id 2020), where turbidity values exceeded 3000 and 5000 NTU, respectively.

The relationship between SSC and turbidity can be approximated by a linear or non-linear model (Gippel, 1995). A linear
115 model assumes a constant relationship between turbidity and SSC, indicating a constant shape and density of the suspended sediments over time, while a non-linear model is preferred in situations where particle size varies with concentration and the relationship between turbidity and SSC is no longer linear (Gippel, 1995). A slightly modified approach applies a log-transformation to the turbidity and SSC data before fitting such a non-linear model (Costa et al., 2018a). One downside of this approach is that back-transformation from the logarithmic to the actual scale requires an additional bias correction function
120 (Duan, 1983) to correct for the larger positive residuals that are a result of the initial log-transformation. In order to find the best SSC-turbidity relationship for our Swiss stations, we fitted a linear model, a non-linear model, and a non-linear model after logarithmic transformation for each station separately, considering simultaneous measurements of turbidity and SSC (with a maximum time lag of 10 min). For all stations, the model performance was the highest for the non-linear model with the form

(Supporting Information Table S1 and Figure S1):

125 $$\text{SSC} = a * \text{Turb}^b, \tag{1}$$

where $Turb$ stands for the turbidity in NTU, a is a characteristic coefficient, and b reflects the effects of systematic variations in particle composition with concentration (Gippel, 1995). The calibrated parameters (a and b) had to be estimated for each catchment individually (Supporting Information Table S2). We computed 10-minute SSC time series for each Swiss catchment by applying these catchment-specific non-linear models to the 10-minute turbidity measurements.

130 Finally, we averaged the Swiss (10-minute) and Austrian (15-minute) SSC data to an hourly time step, as most of the hydro-climatic data are not available at higher temporal resolution. Another benefit of this hourly resolution is that it reduced the influence of single outliers. While we used hourly data for the analysis of extreme SSC events, we further aggregated the data to daily SSC for the analysis of the annual SSC regime. The selected 38 stations all have a time series length of 10 to 12 years within the period 2009–2023.

135 ### 2.1.2 Hydro-climatic data

In addition to the SSC data, we also obtained some other hydro-climatic datasets from different sources. The Austrian Hydrographic Service and the Swiss FOEN provided observational discharge measurements for the 38 stations, which we use at an hourly time step. Hourly precipitation data were available based on a geostatistical combination of rain gauge measurements and radar estimates for Switzerland (CombiPrecip provided by MeteoSwiss at a 1 km^2 resolution and available for 2005–2024,
140 (Gabella et al., 2017)) and for Austria (INCA provided by the Central Institute for Meteorology and Geodynamics (ZAMG) at a 1 km^2 resolution and available for 2007–2018, (Haiden et al., 2011)).

Gridded daily snowmelt and ice melt at a 30 arcsec (approx. 1 km at the equator) resolution were simulated with the gridded global hydrological model PCR-GLOBWB 2.0 (Sutanudjaja et al., 2018; Hoch et al., 2023) for the period 1990-2019. This model was adapted and evaluated for the Alps by Janzing et al. (2024) and contains an updated snowmelt routine (with an
145 expanded temperature index model and regional calibration) and a new glacier routine. In addition to snow- and glacial melt, we calculated daily percentages of snow-free and snow-covered areas for each catchment from snow water equivalent (SWE) data generated by the PCR-GLOBWB 2.0 model, where a grid cell is assumed to be free from snow when SWE < 0.1 mm.

Another variable of interest is soil moisture, as partly saturated soils result in more surface runoff and therefore erosion and the input of fine sediment. Very saturated soils could be less stable and more prone to landslides (Godt et al., 2009; Gariano and
150 Guzzetti, 2016). Daily liquid volumetric soil moisture is obtained from the gridded Copernicus European Regional ReAnalysis Land (CERRA-Land) dataset (Verrelle et al., 2022), which has a high temporal and spatial resolution of 3 h and 5.5 km, respectively, for the period 1984-2021.

2.2 Catchment and seasonally varying characteristics

Characteristics that are relevant for suspended sediment dynamics in rivers can be divided in two groups: (i) catchment char-
155 acteristics (such as geology, elevation, and mean annual temperature) that explain the variation in the SSC regimes between

catchments and (ii) seasonally varying characteristics (such as precipitation and snowmelt) that explain the inter-event variability in SSC within one catchment.

2.2.1 Catchment characteristics

Catchment characteristics include physiographic characteristics, such as elevation, but also hydro-meteorological characteristics, such as mean daily temperature averaged over the available time series length during the period 2009-2023. These characteristics can either control or affect the sediment transport processes or the sediment availability in a catchment. Characteristics related to sediment transport are for example the fraction of glacier cover, the slope, runoff-ratio, mean daily discharge, and mean daily precipitation. Characteristics related to sediment availability are for example the land cover types and geology classes that are present in the catchment. Figure S2 and S3 in the Supporting Information provide an overview of all catchment characteristics that we considered in this study. Some of these characteristics were provided by the large-sample hydrological data sets Camels-CH (Höge et al., 2023) and LamaH-CE (Klingler et al., 2021) and others have been added based on our own calculations. For example, we grouped the 13 geology classes, as defined by GLiM (Hartmann and Moosdorf, 2012), in three groups based on their erodibility index (Alps in Table 1 of Moosdorf et al. (2018)): a low, median, and high erodible geology class. In addition, we calculated the elongation ratio, stream density and meandering index in QGIS based on the DEM (Copernicus, 2013) and catchment delineations, to capture information on fluvial geomorphology (for detailed explanation of these characteristics, see Supporting Information Figure S2 and S3). Finally, we calculated the percentage of the catchment area that was located upstream of big lakes and (hydropower) reservoirs ($> 1 \text{ km}^2$) as these regions might contribute less to the SSC in rivers when sediments get trapped or settle in those larger water bodies.

2.2.2 Seasonally varying characteristics

Seasonally varying characteristics capture inter-event variability and can also be divided into those related to sediment transport and those related to sediment availability. An important catchment characteristic that changes per SSC event and affects the sediment availability is the actively contributing drainage area. We adopt the definitions by Li et al. (2021) and Schmidt et al. (2022) by considering snow-free areas to be potentially erodible. Other seasonally varying catchment characteristics of interest are changes in soil moisture and changes in sediment availability (depletion and replenishment of sediment sources). Seasonally varying hydro-climatic characteristics that relate to sediment transport processes are hourly and daily (erosive) precipitation, snowmelt, ice melt, and river discharge. Because of data scarcity and the relatively short time series, we have decided to not explicitly consider the effect of land-use changes, although potential effects of such changes might be indirectly represented in the time series of soil moisture and discharge. Figure S4 in the Supporting Information provides an overview of all seasonally varying characteristics considered in this study.

2.3 Spatial and seasonal differences in the annual sediment regime

To explain spatial and seasonal variations in the annual SSC regime among catchments, we made use of hierarchical clustering. The methodology comprised several steps which are discussed in more detail below: (i) defining magnitude-shape-timing (MST) indicators that characterise variations in the annual median SSC regime, (ii) clustering the catchments based on these MST indicators, and (iii) identifying the most relevant catchment characteristics that explain the variation in annual SSC regimes.

2.3.1 Indicators used to describe the annual SSC regime

The median annual SSC regime is defined as the 50th percentile of mean daily SSC, smoothed over a 30-days time window to limit the sensitivity of the annual SSC regime to single values. Next, we selected five indicators that are able to capture the variations in magnitude, shape and timing of the annual SSC regime, referred to as MST-indicators (Table 1 and Figure 1a). The magnitude is represented by the median annual SSC per catchment (*SSC_mean*). Shape indicators include the number of peaks (*Peak_numb*) and the relative magnitude difference between the highest and second highest peak (*Peak_magdiff*). Timing indicators include the day of the year (*Peak1_doy*) on which the highest peak occurs and the time difference in days between the highest and second highest peak (*Peak_timediff*). The main peaks were identified automatically with the *scipy.signal.find_peaks* package (Virtanen et al., 2020) based on three criteria: peaks only occur above the 75th percentile of the annual SSC regime; the minimal horizontal distance between peaks is 30 days (one month); and the peak prominence, which "measures how much a peak stands out from the surrounding baseline of the signal and is defined as the vertical distance between the peak and its lowest contour line" (Virtanen et al., 2020). In our case, the peak prominence is catchment specific and defined as 5 % of the SSC range ($0.05 * (SSC\_max - SSC\_min)$). These parameters for peak identification were selected after visual inspection, with at least one peak identified per SSC regime and without selecting too many additional peaks that did not contribute to the overall shape. The number of identified peaks varied from one to three peaks per annual SSC regime. For the catchments with multiple peaks, we also calculated the time lag and relative magnitude difference between the highest and second highest peaks. When the time difference (*Peak_timediff*) has a positive value, the highest peak happens earlier in the year than the second highest peak, and vice versa.

2.3.2 Hierarchical clustering based on SSC regime indicators

We applied hierarchical clustering to cluster the catchments based on their MST-indicators. Clustering started by computing the Euclidean distance matrix, using the matrix of $n = 38*5$ standardized MST indices (python package *sklearn.preprocessing.StandardScaler*). Next, we used a hierarchical clustering algorithm (python package *sklearn.cluster.AgglomerativeClustering*), that allows for non-elliptical clusters, and the Ward variance minimization algorithm, which minimizes the total within-cluster variance (Ward Jr., 1963), to identify clusters of similar SSC regimes. Finally, we optimized the number of clusters (k) by applying the silhouette score and the elbow method, and validated the clustering based on a visual inspection of the dendrogram, keeping in mind the interpretability of the clusters. A sensitivity analysis showed that this clustering approach is robust and that

Table 1. Overview of the five selected MST-indicators that reflect the magnitude, timing and shape of the median annual SSC regime per catchment.

	Indicator	Description
Magnitude	SSC_mean	Mean daily SSC based on the annual 50th percentile SSC regime.
Shape	Peak_numb	The number of main peaks (values between 1 and 3).
	Peak_magdiff	The relative magnitude difference between the highest peak and the second highest peak (note: only if Peak_numb >1), by dividing the absolute difference derived by the range of the SSC regime: (Peak1_ssc - Peak2_ssc) / (SSC_max - SSC_min)
Timing	Peak1_doy	The day of the year (doy) with the highest SSC peak.
	Peak_timediff	The time difference in days between the highest peak and the second highest peak (note: only if Peak_numb >1).
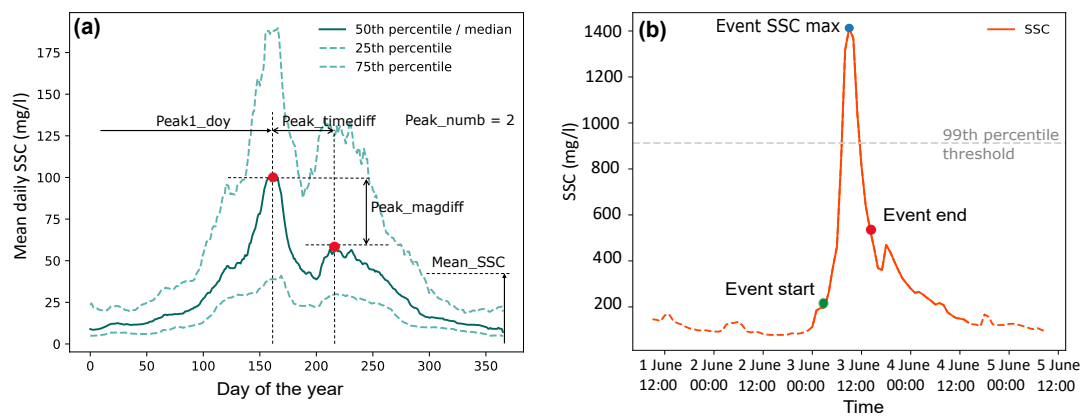
Figure 1. (a) Visual overview of the five selected MST-indicators (explained in Table 1) in relation to the median annual SSC regime of one example catchment. (b) SSC event (with event start and end), where the SSC max is exceeding the 99th percentile threshold.

removing single or multiple catchments does hardly influence the clustering results. Furthermore, a comparison with clusters derived by k-means clustering showed that the final clusters identified are relatively stable, regardless of the choice of the clustering technique.

2.3.3 Interpretation of variation in SSC regimes based on static catchment characteristics

For the interpretation of the three SSC regime clusters, we selected a number of physiographic catchment characteristics and hydrometeorological attributes (Section 2.2.1), that may be able to explain the spatial and seasonal variations in annual SSC regimes in mountain rivers. To better compare these characteristics among the different catchments, we used area-independent values, such as percentages (e.g. % forest cover) and specific discharge (in mm d^{-1}). In addition, we normalized all catchment-

225 and hydro-meteorological attributes to the range 0-1 across all catchments. For each cluster, we identified the most important catchment characteristics that are able to explain the spatial variation between different annual SSC regimes. The most important characteristics are those that clearly differ for the selected clusters and thus support the clustering. Finally, we also compared the annual regimes of the main transport processes (precipitation, glacial melt, snowmelt, and discharge) with the annual SSC regimes.

2.4 Spatial and temporal variations in extreme SSC events

230

To identify different types of extreme SSC events and explain the spatial and temporal occurrence of these events, we performed several analysis steps which are discussed in more detail below: (i) detecting extreme SSC events, (ii) designing a classification scheme to distinguish between event types, and (iii) explaining the spatial and temporal differences between SSC event types based on seasonally varying characteristics, event characteristics, and antecedent conditions.

2.4.1 Detection of extreme SSC events

235

Extreme SSC events, i.e. episodic peaks of suspended sediment concentration, can be defined in different ways. While there is no commonly used definition for SSC extreme events, the peak-over-threshold method is widely used to extract extreme events (Skålevåg et al., 2024; Hamshaw et al., 2018; Haddadchi and Hicks, 2021; Blöthe and Hoffmann, 2022). In this study, we defined SSC extreme events as events for which the peak value exceeds a locally defined 99th percentile threshold (Figure 1b).

240 We identified the start of the event based on a rapid increase in the slope of SSC prior to the SSC peak (the increase in slope [Δ mg L^{-1}] is larger than the difference between the 50th and 75th percentile of SSC for that catchment [mg L^{-1}]). The end of the event is defined as the time when the SSC drops below 0.4 times the SSC peak value. We also tested and compared other definitions, where the end of the event was equal to crossing the 90th percentile or was determined based on the decrease in slope. However, a sensitivity analysis showed that the choice of the exact definition had a limited effect on the total number of

245 events selected (Supporting Information Figure S5 and Table S3). When the end of one and the start of the next event are less than 12 hours apart, these events were merged into one event, because we assumed that these events share the same drivers. We have deliberately chosen to make the selection of SSC events independently of discharge because such an approach also enables the selection of extreme SSC events during low flow periods. Events with missing SSC or hydro-climatic data are removed. Since daily snowmelt and ice melt data was only available until the end of 2019, this means that we did not include

250 extreme events that occurred after this date. Our approach led to the extraction of 2398 SSC extreme events across the entire study domain, with on average 64 events per catchment (min = 10, max = 143).

2.4.2 Classification of extreme events based on their dominant transport process(es)

To distinguish between different types of extreme events, we developed a classification scheme that identifies the most important driver(s) of each event. The three hydro-climatic processes that are most important for sediment transport to the river are

255 erosive rainfall, snowmelt and glacial melt (Costa et al., 2018a). We assumed that each event is caused by either one or two

out of these main transport processes. Inspired by the event-based classification of flood generation processes by Stein et al. (2020), we developed a classification scheme for extreme SSC events that assigns each event to one out of nine event types (Figure 2). The most dominant transport process(es) per event is (are) determined based on the total rainfall, snowmelt and glacial melt during the 24 hours prior to the SSC peak of the event. Costa et al. (2018a) found that a 1-day time lag is the most relevant time lag for predicting SSC for the Rhône catchment. We tested this time lag on a selection of events and found that this short time lag aligns well with the fast response time of our catchments. Furthermore, we distinguished between high- and low-intensity precipitation as two different driving processes, because soil erosion by runoff depends on rainfall intensity (Parsons and Stone, 2006; Mohamadi and Kavian, 2015). Precipitation is considered high intensity if the maximum hourly precipitation during the 24-hour time window exceeds the catchment-specific 99th percentile threshold of hourly precipitation. All other precipitation values are considered low intensity. According to our definition, an event had two dominant transport processes (e.g. precipitation and snowmelt driven) if both precipitation and snowmelt contributed more than 1/3 of the total water input. The threshold of 1/3 was chosen to allow for a maximum of two dominant processes per event. A lower threshold could result in the selection of all three drivers for an event, but information about which of the drivers is the most dominant would be lost. A sensitivity analysis showed that higher thresholds (of up to 1/2) result in a larger number of events with only one dominant transport process. Because we were also interested in events with compounding drivers, we used the 1/3 threshold.

2.4.3 Event characteristics and antecedent conditions analysed per event type

To learn more about the differences and similarities between the nine event types, we also looked at the spatial and temporal distribution of the event types across the Alps, the effect of antecedent conditions, and whether events belonging to the same event type share the same event characteristics. Event characteristics include event duration, mean and maximum event SSC, specific suspended sediment yield (sSSY) [t km^{-2}], and event complexity, defined as the number of peaks in the SSC between the start and end of the event (Figure 1b). We also calculated the sSSY event fraction out of the mean annual sSSY per catchment as an indicator for the extreme nature of the event in terms of the sediment load transported. In addition, we monitored important seasonally varying antecedent conditions during the two days prior to the SSC event, such as the mean snow cover and the soil moisture in the catchment, which control sediment availability.

Finally, we investigated the role of long-term catchment memory in terms of sediment availability on the development of extreme events. As a proxy for sediment memory, we compared the long-term cumulative sSSY prior to each event with the catchment specific mean annual cumulative sSSY curve (for a detailed explanation see Figure S6 in the Supportive Information). For each day of the year, we determined whether the cumulative sSSY was above or below the mean annual sSSY curve. If the cumulative sSSY was below the mean (=negative deviation), less sediment than usual has been transported during that season and therefore more sediment may be available for mobilization during upcoming events. If the cumulative sSSY was above average (=positive deviation), more sediment than usual had already been transported by previous events, which may have led to sediment depletion in the catchment and limited sediment availability for the next events. To make this index com-

Figure 2. Decision tree used to categorise extreme SSC events into one out of nine predefined event types. The most dominant transport process(es) is (are) determined based on the fraction of total rainfall (P), snowmelt (S) and ice melt (I) (also referred to as glacial melt) compared to the total sum of P, S and I (Tot) during the 24 hours prior to the SSC peak of the event. Precipitation is classified as high intensity (high int.) if the maximum hourly precipitation (P1h) during the 24-hour period exceeds the catchment-specific 99th percentile threshold of hourly precipitation. Otherwise it is classified as low intensity (low int.).

parable among catchments, we standardized the deviation of the long-term cumulative sSSY from the catchment specific mean annual sSSY curve by dividing it by the catchment annual mean cumulative sSSY.

3   Results

3.1   Large variation in median SSC among catchments

We observe a large variation in median SSC among the different catchments, with some catchments showing a median SSC which is a hundred times greater than the one of other catchments, even though all catchments are located in the same mountain range (Table 2). The median SSC varies from 2 mg L^{-1} to 229 mg L^{-1} between the 38 catchments, with a mean SSC value of 27 mg L^{-1} on average. The mean annual sSSY varies from 23 t km^{-2} yr^{-1} to 1415 t km^{-2} yr^{-1}, again with a difference of 2 orders of magnitude. The mean annual sSSY averaged over all 38 catchments is 277 t km^{-2} yr^{-1}. The catchment with the largest

Table 2. Statistical description of the variation in the annual SSC regime (median and maximum) and cumulative annual sSSY among the 38 catchments.

	Averaged over all 38 catchments		
	Median SSC-regime (mg L^{-1})	Max SSC-regime (mg L^{-1})	Annual sSSY (t km^{-2} yr^{-1})
Min	2	4	23
Median	17	88	227
Mean	27	164	277
Max	229	1082	1415

median SSC and sSSY is the Vent catchment located in the Ötztal (Austria). This catchment has the highest mean elevation (2889 m.a.s.l.), a glacier cover of 30 %, and is know for its high sediment output (Schmidt et al., 2022; Skålevåg et al., 2024). The catchment with the lowest median SSC is located at the foots of the northeastern Austrian Alps with a mean catchment elevation of 938 m.a.s.l.. The large spatial variability allows us to investigate the causes of variation between catchments. To do this, we group the catchments into different clusters and analyse these clusters separately.

3.2 Three types of annual SSC regimes

Our hierarchical clustering approach identified three main types of annual SSC regimes, based on the magnitude, the shape and the timing of the peak(s) (Figure 3 a-c): SSC regimes in Cluster 1 ($n = 12$) have two or multiple peaks, where the highest peak occurs at the end of spring and earlier in the year than the second highest peak; SSC regimes in Cluster 2 ($n = 7$) generally have one main peak, which occurs in mid-summer; and SSC regimes in Cluster 3 ($n = 19$) show an opposite shape compared to Cluster 1, with the highest peak occurring later in the year than the second highest peak. The number of peaks and the timing of the first peak are the most important indicators for dividing the annual SSC regimes into these clusters, while the magnitude of the SSC regime (median SSC) is considered the least influential for clustering the catchments.

The catchments belonging to the three different SSC clusters are characterized by substantially different catchment characteristics (for an important subset see Figure 4a-h and for the full overview see Supporting Information Figure S7). The catchments that belong to Cluster 2 can be described as high-elevation, small mountain catchments because they are characterised by high mean elevation and slope, a high fraction of glacier coverage, high mean daily snowmelt and glacial melt, and a high fraction of sand (dark brown boxplots in Figure 4a-h). The effect of reservoirs is limited and none of the catchments are located downstream of big lakes (Supporting Information Figure S7). The catchments belonging to Clusters 1 and 3 have quite similar catchment characteristics (beige and turquoise boxplots in Figure 4a-h). Compared to those in Cluster 2, they have a larger area, a lower mean elevation and a higher fraction of clay and silt. The catchments in Cluster 1 have in general a smaller fraction of precipitation that falls as snow, and the day of the year on which the catchment is completely snow-free happens earlier in the year than for the catchments in Cluster 3. The fraction of highly erodible geology (such as unconsolidated sediments) is higher in catchments belonging to Cluster 1, while the catchments in Cluster 3 have a larger fraction of low erodible
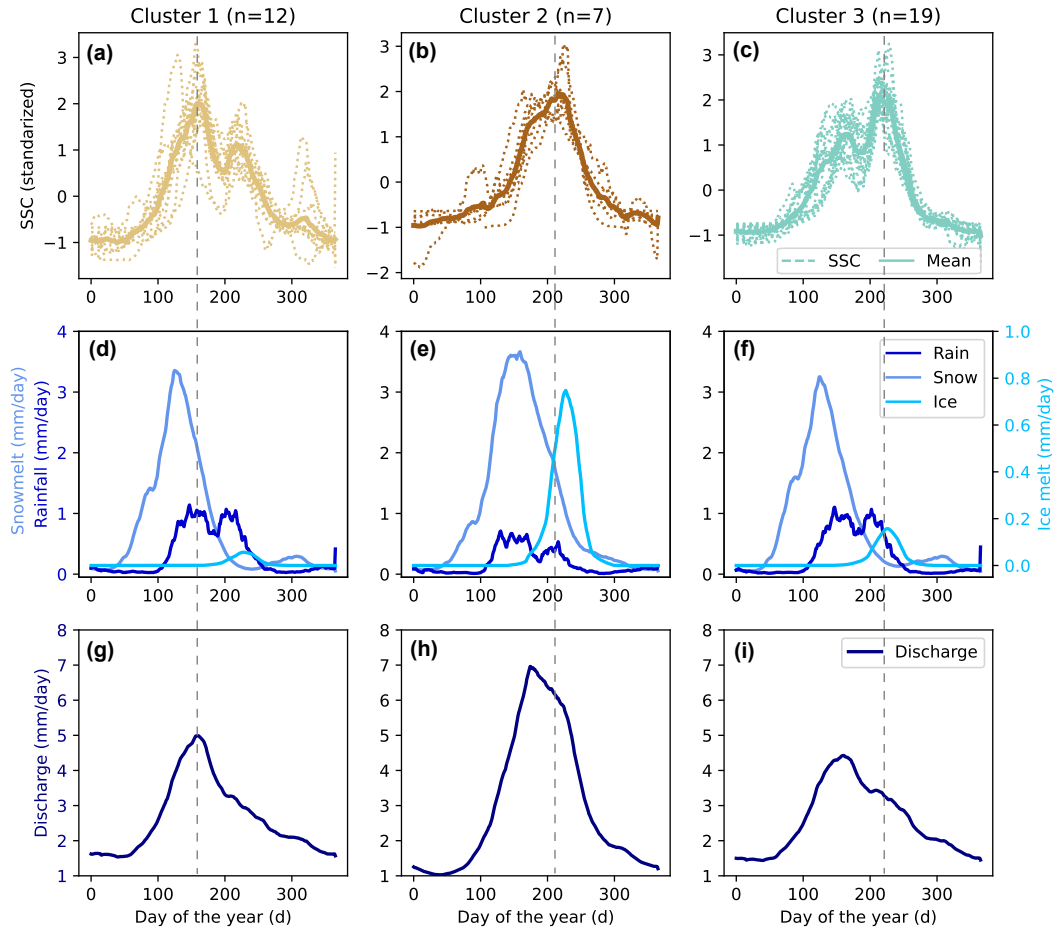
Figure 3. The median SSC regimes (standardized by removing the mean and scaling to unit variance) can be grouped into three different clusters: (a) Cluster 1 (n=12), (b) Cluster 2 (n=7), and (c) Cluster 3 (n=19). The dashed lines show the regimes for the n individual catchments that belong to that cluster and the bold line is the mean of all catchments per cluster. Panels d, e, and f show the mean annual regimes of precipitation, snowmelt, and glacial melt averaged in mm/day over all catchments within a cluster. The mean annual discharge regime over all catchments within a cluster is given in panels g, h, and i. The grey vertical dashed lines spanning panels indicate when peak SSC occurs.

geology (e.g., plutonic rocks, carbonate sedimentary rocks, acid volcanic rocks). Finally, a larger fraction of the catchments in Cluster 1 than Cluster 3 are located upstream of lakes and reservoirs (Supporting Information Figure S7).

The subtle differences between catchments in Clusters 1 and 3 become more pronounced when we compare the annual SSC
325   regimes with the mean annual regimes of precipitation, snowmelt and glacial melt per cluster (Figure 3d-f). Catchments with a single-peak SSC regime (Cluster 2) are characterised by late snowmelt (as high mean elevation results in a late melting season), immediately followed by a significant input from glacial melt. The catchments in Clusters 1 and 3 also receive significant snowmelt, but the melting starts at least one month earlier in the year than for catchments in Cluster 2. The first peak in SSC

for Clusters 1 and 3 is mostly aligned with the first peak of rainfall. The largest difference between the catchments of Cluster 1 and 3 is the amount of glacial melt during late summer. In catchments belonging to Cluster 3, the glacial meltwater peak perfectly coincides with the second and highest SSC peak of the annual SSC regime. In catchments belonging to Cluster 1, this increase in SSC during peak glacial melt is also visible, but much weaker than for those in Cluster 3. In terms of annual peak discharge (Figure 3g-i), catchments in Cluster 1 show peak discharges approximately simultaneously with the peak SSC, while peak discharge for catchments in Cluster 3 is out of phase with the SSC peak. The spatial distribution of the different catchments across the Alps (Figure 4i) supports the above findings. Catchments belonging to Cluster 2 are mainly located in the higher alpine region (with one exception located in eastern Austria). The catchments of Cluster 3 follow a clear line from east to west and are bounded to the north and south by the less mountainous catchments of Cluster 1.

The magnitude of the SSC regime, although not used as such to split the catchments into the above-mentioned three clusters, has a moderate correlation (Pearson correlation coefficient >0.5) with a number of catchment characteristics (Figure S8 in the Supporting Information). The median SSC has a moderate positive correlation with the mean daily snowmelt (0.67), mean daily snow cover (0.67), catchment elevation (0.64), runoff ratio (0.60) and sand fraction (0.58), fraction of precipitation that falls as snow (0.57), fraction of glacier coverage (0.55) and mean daily glacial melt (0.49). A negative correlation is found between the median SSC and the fraction of forest cover (-0.64), mean daily soil moisture (-0.58), fraction of silt and clay (-0.58) and the mean daily air temperature (-0.58). These findings suggest that higher median SSC values should in general be expected in higher elevated catchments that have a large contribution of snow and ice.

3.3 Temporal and spatial occurrence of the nine event types

In total, we extracted 2398 extreme SSC events, of which rainfall is by far the most dominant driver. In total, 85 % of the events are purely caused by either high- or low-intensity rainfall (1562 events (65.1 %) and 506 events (21.1 %)) (Figure 5a and c). Those rainfall-driven events occur all year round, but with a higher frequency during summer. Snowmelt-driven events are restricted to the melting season and occur only during late spring and autumn, and their timing is also dependent on catchment elevation. The same is valid for events that are caused by glacial melt, which only occur during July and August, when the snow cover on glaciers is minimal and the glacier becomes susceptible to melting. In total, 11 % of the events are (partly) snowmelt driven and only 3.1 % are (partly) glacial melt driven.

The proportion of snow- and glacial melt-dominated events is significantly higher for high-elevation and partially glacierised catchments, which belong to Cluster 2 based on the annual SSC regime clusters. In these catchments, snow- and glacial melt-dominated events account for almost 35 % of all events (Figure 5b). In contrast, lower elevation and larger catchments (Clusters 1 and 3), show many fewer melt-dominated events (< 10 % out of all events).

3.4 Event type characteristics

The event characteristics, such as the event maximum SSC, the area-specific suspended sediment yield (sSSY), and the sSSY event fraction out of the annual mean sSSY, vary greatly among the different event types (Figure 6 and Figure S8 in Supporting Information). Nine out of the ten most extreme events, with the highest peak SSC, occurred in summer and are caused solely
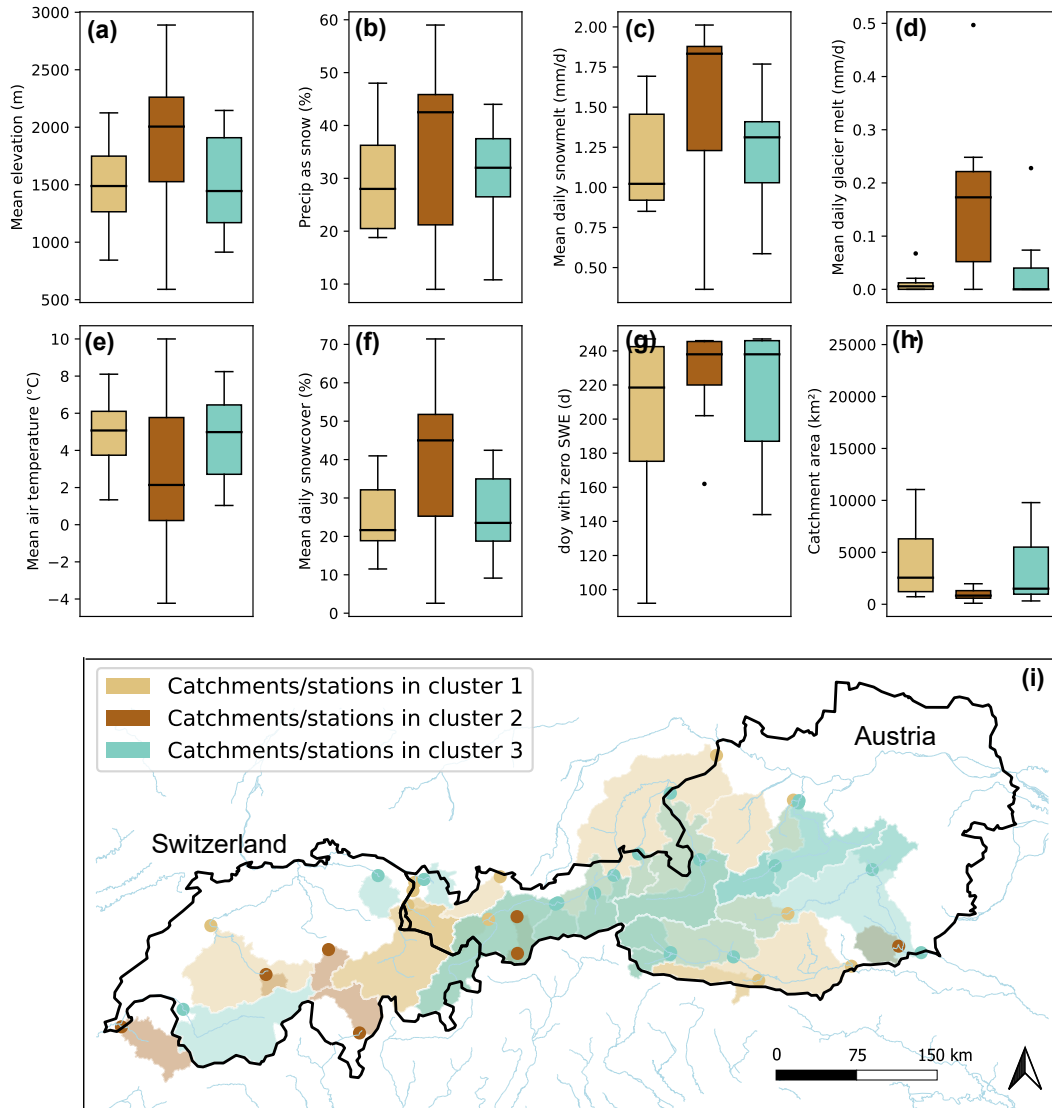
Figure 4. Panels (a-h) illustrate eight static catchment characteristics and their distribution across the three different clusters and within each cluster (the internal distribution is visualised by the boxplots). Panel (i) maps the spatial location of the (nested) catchments over Switzerland and Austria.

by high-intensity rainfall (peak SSC = 118 g L^{-1} and sSSY event fraction = 0.33, averaged over the 10 most extreme events) (Figure 6a). Similarly, also the events with the highest sSSY and sSSY event fraction are caused by high-intensity rainfall (Figure S9a in Supporting Information). However, when we look at the median of all events per event type, other event types result in higher peak SSC (Figure 6j) or high sSSY event fractions (Figure S9j in Supporting Information). On average, the
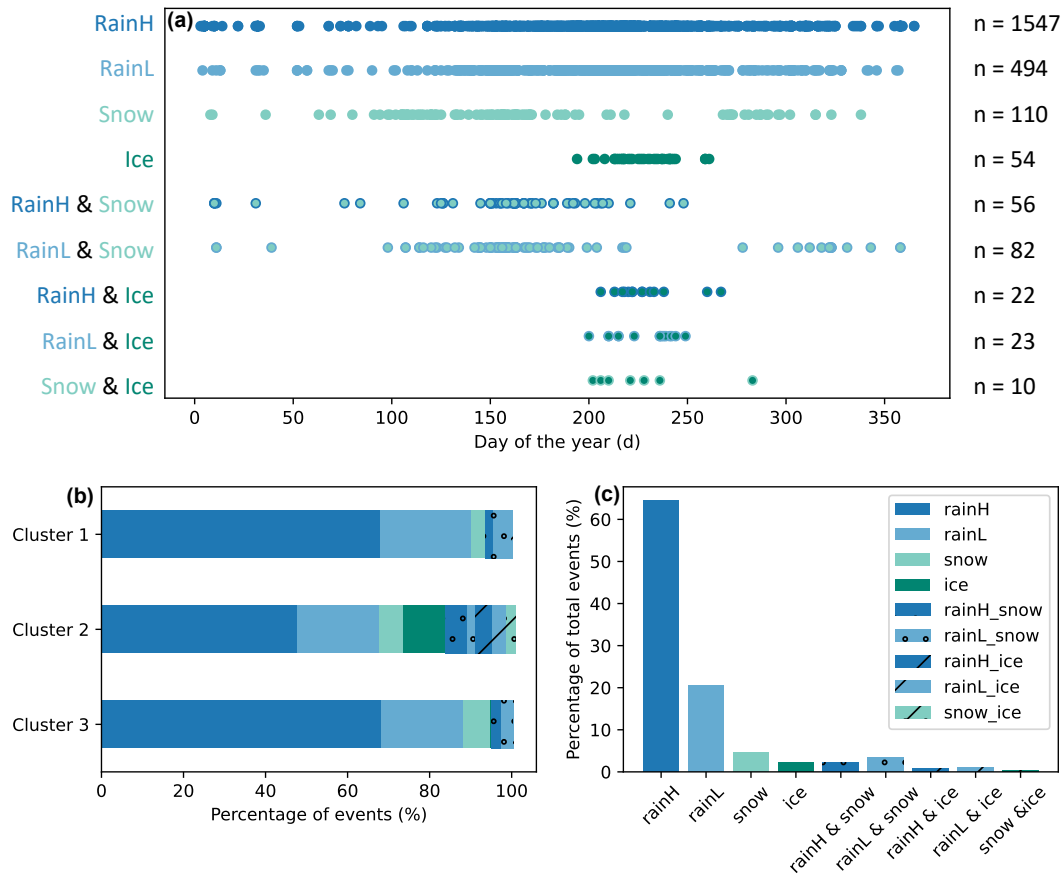
Figure 5. (a) Seasonality of occurrence of the nine event types: high intensity rainfall (RainH), low intensity rainfall (RainL), snow melt (Snow), glacial melt (Ice), or a combination of two of the above mentioned transport processes. The total number of events is 2398. (b) Proportion of event types for each of the three annual SSC clusters. (c) Percentage of events per event type compared to the total number of observed events.

highest peak SSC values are caused by events with compounding drivers, namely those that are caused by a combination of glacial melt and high intensity rainfall (median peak SSC of 5.5 g L^{-1}). Events caused by glacial melt alone lead on average to the second highest suspended sediment concentrations (median peak SSC of 4.2 g L^{-1}), the highest specific yields (median sSSY of 32 t km^{-2} per event), and the second highest fraction of event sSSY (median sSSY event fraction of 0.03). Other event 370 characteristics, such as the mean duration of events and the event complexity (number of peaks per event) are less informative as they do not clearly stand out for single event types. All events have a relatively short duration of less than one day, with a mean duration of 17 hours.

In addition to the characteristics of the events, we also considered the antecedent conditions, such as the liquid volumetric soil moisture and snow cover, during the two days prior to the event. In general, the majority of events occurs when snow
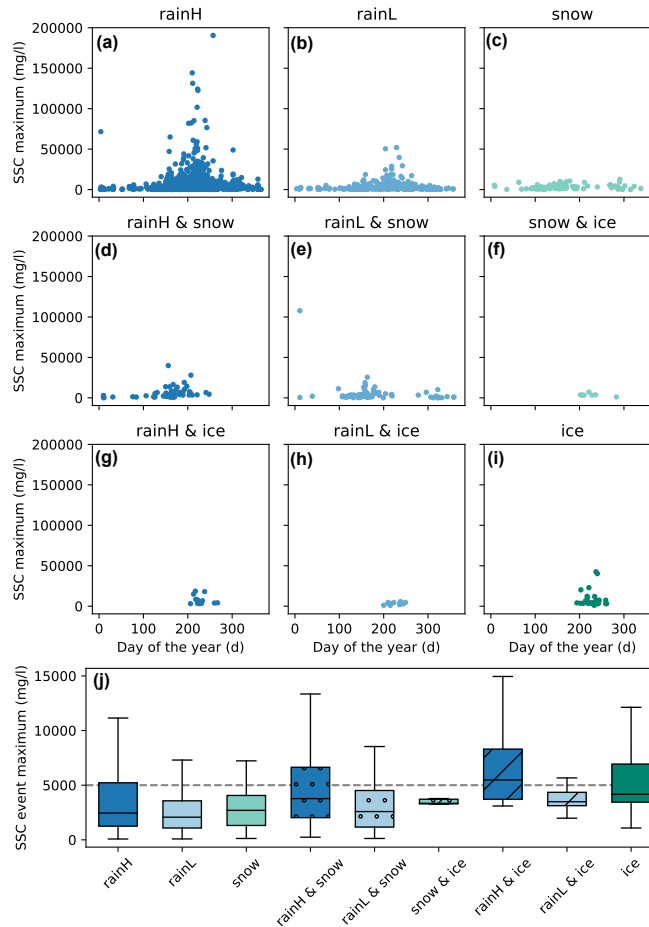
Figure 6. Relationship between event magnitude (peak SSC) and generation processes. Panels (a-i) illustrate the variation of peak SSC (including outliers) over time per event type. Panel (j) illustrates the distribution of peak SSC (without outliers) for each event type, with the median value represented by a horizontal grey line.

cover is minimal or absent (Figure 7a). However, a more detailed examination of the various event types provides additional insights (Figure S10 in Supporting Information). Events that are partly or entirely driven by glacial melt occur only when the snow cover has disappeared or is at least smaller than 30 %. In contrast, snowmelt events require the presence of a snow pack, and extreme SSC events occur under both limited and extensive snow cover. Events driven by a combination of rainfall and snowmelt are most prevalent when the snow cover is between 10 % and 30 %. However, some particularly severe events have been observed with a snow cover of 40 % to 70 %. Despite the occurrence of some of the most extreme events with exceptionally high peak SSC values under conditions with minimal snow cover, no clear pattern or relationship between snow cover and SSC could be identified.
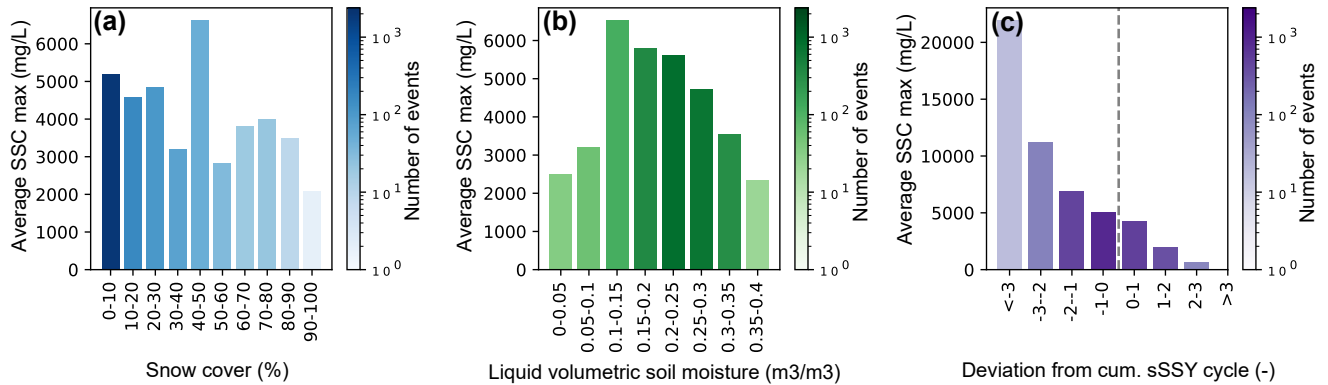
Figure 7. Antecedent conditions prior to the extreme SSC events are given for (a) snow cover, (b) liquid volumetric soil moisture, and (c) the deviation of the daily cumulative sSSY from the annual mean cumulative sSSY regime. Per interval, the bars show the peak SSC averaged over all the events that belong to each of the intervals. The colour saturation is an indication for the number of events (in log scale) that belong to each interval. Dark colours mean that more events belong to that interval. Snow cover prior to the event can vary from 0 to 100 %. The liquid volumetric soil moisture generally varies from 0 to 0.4 m^3 m^{-3}. The deviation from the cumulative sSSY regime can either be negative (indicating more sediment availability than usual) or positive (indicating potential sediment depletion).

The majority of events occurs when liquid volumetric soil moisture lies between 0.2 and 0.3 m^3 m^{-3} (Figure 7b). The maximum liquid volumetric soil moisture typically ranges from 0.2 m^3 m^{-3} in sandy soils to 0.4 m^3 m^{-3} in clay soils. A more detailed overview per event type is visible in Figure S11 in the Supporting Information, which shows some discrepancies in the relation between peak SSC and soil moisture between the event types. Glacial melt events predominantly occur under liquid volumetric soil moisture values of 0.2-0.25 m^3 m^{-3}, with occurrences at lower or higher soil moisture levels being rare. In high-elevation and partly glacierized catchments, where glacial melt events are most frequently observed, the soil is typically composed of a higher proportion of sand, which may contribute to the observed lower liquid volumetric soil moisture. In the case of rainfall-driven events, the most severe events, with the highest peak SSC, take place under antecedent soil moisture values between 0.1-0.2 m^3 m^{-3}, which implies rather dry conditions. The statistical analysis revealed no significant correlations between soil moisture and SSC.

The proxy for catchment memory and sediment availability, designed as the deviation of the long-term cumulative sSSY from the mean annual cumulative sSSY regime, shows that more (severe) events occur when the deviation is negative (Figure 7c). A negative deviation indicates a situation in which the transport of sediments during the period prior to the event was below the expected level, suggesting that sediment availability is not a limiting factor for riverine sediment transport. More negative deviations result in larger observed peak SSC. Similar patterns are observed for rain and snow dominated events, an exception being (partly) glacial melt events (Figure S12 in Supporting Information). A significant number of glacial melt events occur when the deviation is slightly positive (Figure S12f-i in Supporting Information).

4 Discussion

4.1 Mean SSC regimes

Our results show that the annual SSC regimes can be divided into three clusters (Figure 3a-c), where the catchments in each cluster share similar catchment attributes (Figure 4a-h) and seasonal regimes of snow- and glacial melt (Figure 3d-i). This suggests that, in addition to precipitation, the amount of glacial melt and the magnitude and timing of snowmelt strongly control the shape of the annual SSC regime (number of peaks) and the timing of SSC peaks (Figure 3d-i). This is particularly evident when examining catchments in Cluster 3, for which the occurrence of the glacial meltwater peak perfectly coincides with the second and highest SSC peak in the annual SSC regime (Figure 3c and f). The importance of snow- and glacial melt is confirmed by the analysis of the catchment characteristics (Figure 4a-h). The most important characteristics explaining seasonal sediment dynamics are those that influence the magnitude and timing of snow- and glacial melt, for example, the presence of glaciers (even if they cover only a small part of the catchment), catchment elevation, the proportion of precipitation falling as snow, and catchment area. The importance of meltwater for SSC has already been highlighted by multiple other studies, for example: Costa et al. (2018b) showed that glacial melt produces the highest SSC per unit runoff, Buter et al. (2022) showed that glacial melt results in even higher sediment concentrations than snowmelt, and Li et al. (2024) showed that the suspended sediment yield of glaciated catchments can be an order of magnitude larger than that of glacier-free catchments.

The high concentration of suspended sediment in glacial meltwater can be explained by the importance of the glacier and glacier forefields as a sediment source and temporary storage. Glacial abrasion on the bedrock causes erosion and these sediments get transported by subglacial channels. However, these channels need time to develop at the start of the ablation season before they become very effective (Swift et al., 2005). In addition, a lot of material is stored in the recently deglaciated moraines and the glacial forefields (Moore et al., 2009). The braided stream network in this deglaciated terrain can be highly dynamic and therewith has an important influence on sediment availability (Mancini et al., 2024). This means that areas above 2500 m.a.s.l., which are characterized by glacier tongues, bare rock surfaces and recently deglaciated areas, are crucial for sediment generation in high-altitude catchments (Schmidt et al., 2022). A sudden release of suspended sediments has been observed when areas above 2500 m become snow-free and the sediments are no longer protected from mobilization by the snow cover (Schmidt et al., 2022).

In addition, our results show that the relationship between SSC and discharge is not straightforward because the annual discharge regime is completely out of phase with the SSC regime in some catchments (Figure 3), in particular in catchments that belong to Cluster 3 and are characterised by significant glacial melt input during late summer. Discharge has long been considered one of the key predictors of SSC, and the relation between discharge and suspended sediment concentration forms the basis of the well-known sediment rating curves and hysteresis analyses (Walling, 1977). However, other studies have recently shown that this relationship has been overvalued (Costa et al., 2017; Schmidt et al., 2023; Skålevåg et al., 2024). Sediment rating curves are characterised by a large variability of observations around the regression curve, which can span one or several orders of magnitude, and they tend to underestimate (overestimate) SSC during high (low) discharge (Walling, 1977; Horowitz, 2003; Asselman, 2000). One of the major limitations is that the Q-SSC relationship does not explicitly address the sources of

sediment and their activation by different hydro-climatic forcing. Costa et al. (2017) have shown that a sediment source per-
spective using hydro-climatic forcing (rainfall, snowmelt and glacial melt) is more appropriate to explore sediment dynamics
than traditional discharge-based rating curves. In line with this, Zhang et al. (2021) introduced a sediment-availability-transport
model that captures the time-varying sediment availability. Their results are consistent with ours, as our results suggest that the
origin of water entering the river system is more informative for understanding the mean annual SSC regime than the absolute
magnitude of discharge alone.

Even though forcing and transport processes were expected to be among the key determinants of the annual SSC regime, it
is still surprising that catchment characteristics related to sediment availability, spatial connectivity, geology and soil type did
not appear to be more important for explaining the variation in the annual SSC regime among catchments (Figure S6). The
catchments belonging to the three clusters of annual SSC regimes did show some mutual differences in the fraction of clay, silt
and sand, and we observed a slightly larger fraction of highly erodible geology in catchments of Cluster 1 compared to those in
Cluster 3. However, these differences were small and they did not significantly affect the timing and shape of the SSC regime.
We did observe some correlations between a few catchment characteristics and median SSC, but again characteristics related
to snowfall, snow cover, ice and catchment elevation were more important descriptors of SSC behaviour than geology-related
characteristics. While SSC is controlled by the depletion and replenishment of different sediment sources over longer time
scales (Doomen et al., 2008), we hypothesise that these processes were found to be less relevant in our study because our
analyses focused on the mean annual scale.

Looking at the spatial variability of median SSC and sSSY values across catchments, we found that values can vary greatly
across locations (Table 2). Median SSC values range from 2.11 mg L^{-1} to 229 mg L^{-1} per catchment, while the mean annual
sSSY varies from 19 t km^{-2} yr^{-1} to 1226 t km^{-2} yr^{-1}. These values are in line with those previously described in literature,
where sSSY values vary between 100-1000 t km^{-2} yr^{-1} as mountainous regions are generally characterised by high sediment
yields (Blöthe and Hoffmann, 2022; Vanmaercke et al., 2011; Bogen, 2008; Borrelli et al., 2014; Hinderer et al., 2013; Mano
et al., 2009). In addition, Panagos et al. (2015) predicted a mean soil loss rate of 527 t km^{-2} yr^{-1} for the Alpine climate
zone (Alps, Pyrenees, and southern Carpathians), due to the combined effect of rainfall erosivity and topography. One of the
highest sediment discharge rates in Europe was recorded in the Italian Central Apennines, with a specific yield of 3235 t km^{-2}
yr^{-1} (Borrelli et al., 2014), due to very active geomorphological processes such as gully, rill, bank and channel erosion and
re-entrainment of landslide sediments. Such extremely high levels have not been recorded in our catchments.

4.2 Extreme SSC events

From the event classification, we conclude that rainfall is by far the most dominant driver of extreme SSC events (Figure 5c),
which shows that slightly different processes are important for controlling extreme events compared to annual SSC regimes. In
total, 85 % of the events are purely caused by either high- or low-intensity rainfall (1562 events (65.1 %) and 206 events (21.1
%)) (Figure 5c). This dominant role of precipitation in causing extreme SSC has also been highlighted in other studies (Schmidt
et al., 2022; Mano et al., 2009; Lana-Renault et al., 2007; Blöthe and Hoffmann, 2022). The process of rainfall-driven splash
erosion, which is followed by the generation of surface overland flow on hillslopes, results in the delivery of fine sediment

to the river network. Therefore, precipitation is also increasingly considered as a valuable input to various SSC modelling approaches, such as the process-based rating curve of Costa et al. (2018a), the extended sediment rating curve of Wolf et al. (2023), and the machine learning model of Aires et al. (2023). Given that rainfall affects a much larger area than glacial melt or even snowmelt, and occurs at higher intensities, it was anticipated that rainfall would emerge as the most dominant driver. On the other hand, for snow- and glacier-dominated catchments the number of snow- and glacial melt events was larger and could make up to 35 % of all events in these catchments. This is consistent with the existing knowledge on runoff generation processes in mountainous snow-dominated catchments, where snow- and glacial melt are significant contributors to overland flow and river discharge (Muelchi et al., 2021).

From the comparison of mean SSC peak values among the different event types, we conclude that events that are partly or entirely dominated by glacial melt result in relatively high SSC (Figure 6j). These findings are in line with existing literature stating that glacial melt has a significantly higher suspended sediment input per unit of runoff compared to snowmelt and rainfall (Buter et al., 2022; Costa et al., 2017, 2018b). Events with compounding drivers, specifically those resulting from the interaction of glacial melt and high-intensity rainfall, show the highest peak SSC values on average (median peak SSC of 5.5 g L^{-1} and mean peak SSC of 7.7 g L^{-1}). However, the 10 highest SSC values in our data set are predominantly associated with high-intensity rainfall events during the summer season, with values reaching up to 118 g L^{-1}. Although these observed SSC values are extremely high, concentrations in the same order of magnitude have been found by other authors (Schmidt et al., 2022) and in other alpine catchments (Mano et al., 2009). Actually, a significant amount of 573 extreme SSC events (24 % of all extreme events) in our data set causes SSC peak values above 5 g L^{-1}, which are very likely to be harmful or lethal to a large number of aquatic species, including trout, salmon, and aquatic invertebrates (Newcombe and Macdonald, 1991; Kemp et al., 2011; Collins et al., 2011). Such high levels of SSC also degrade drinking water quality, lower the transparency and limit the penetration of sunlight into the water, lead to a degradation of the habitat quality for spawning fish, and clog the gills of fish and other aquatic organisms, which can lead to death (Kemp et al., 2011).

On average, the highest event sSSY is found for events driven by glacial melt (52 t km^{-2}) or a combination of glacial melt and high-intensity rainfall (42 t km^{-2}) (Figure S9 in Supporting Information). During such events, large volumes of sediment produced by glacial erosion and temporarily deposited in proglacial systems are likely to be mobilised and transported downstream by high-intensity precipitation (Li et al., 2024). If we compare the event sSSY with the mean annual sSSY of the catchment, we see that these extreme events transport on average 2 % of the catchment's annual sSSY. However, some high-intensity rainfall events can transport up to 20 % or 60 % of the annual sSSY. Similar results were found for the Vent catchment in Ötztal, where individual summer rainstorm events can account for up to 26 % of the annual sSSY in just over 24 hours (Schmidt et al., 2022).

During some of the most sediment-productive events, some headwater catchments transported more than four times the average annual sSSY in just 6 to 8 days. Further investigation showed that these events were related to two major storm and flood events that occurred in Europe: the large flooding in Central Europe in early June 2013, with more than 300 mm of precipitation over four days on the northern side of the Alps, resulting in large flooding in the Upper Danube basin (Blöschl et al., 2013), and the storm "Vaia" that hit southern Austria on 28 October 2018, characterized by extreme accumulated precipitation of up to 850

mm in three days (Giovannini et al., 2021). Further downstream, the sSSY of these flood events still accounted for up to 150 % to 280 % of the average annual sediment yield. Such high sediment yields are only possible in combination with landslides and river floods, when all the sediment in and near the river bed gets activated. This was the case for both the 2013 and 2018 events (Blöschl et al., 2013; Giovannini et al., 2021). While these events with very high sediment yield play a significant role in soil loss within a catchment, a high sediment yield does not necessarily lead to a high sediment concentration as long as it is combined with high discharge (Zheng et al., 2021).

The relationship between antecedent conditions and extreme suspended sediment concentration (SSC) events is complex. Notably, some of the highest peak SSC and specific suspended sediment yields (sSSY) occurred during periods of high soil moisture and limited snow cover (Figure 7), as saturated soils are generally more prone to landslides and snow free soils are less protected from erosion (Godt et al., 2009; Hamshaw et al., 2018). At the same time, rainfall during previously wet conditions does not always lead to high SSC. Moderate rainfall can also lead to high runoff without a corresponding increase in SSC. If the whole catchment contributes to the runoff, sediment concentrations may not increase due to dilution effects (Lana-Renault et al., 2007) if the sediment input is proportional to the water input. In contrast to wet soils, dry soils can also be prone to erosion at the onset of rainfall events due to hydrophobicity, splashing, and surface sealing (Zambon et al., 2021). Our observations indicate that high-intensity rainfall events often result in more severe SSC under relatively dry conditions compared to wet ones (Figure S11 in Supporting Information). A final complicating factor, which we did not explicitly consider in this study, is the potential effect of changes in land use on soil moisture, discharge, and erosion. All these contrasting signals complicated efforts to establish a clear correlation between SSC and soil moisture (Figure 7b). Furthermore, we noticed that glacial melt occurs only when the snow cover has disappeared or is at least smaller than 30 %. This could be a model artefact, as it is consistent with how glacial melt is represented in the PCR-GLOBWB 2.0 model, which assumes that glaciers only start melting when they are no longer covered (and protected) by snow. This assumption is supported by findings of Schmidt et al. (2022), who showed that subglacial sediment sources are inactive as long as areas above 2500 m (including glacier tongues) are frozen or snow-covered, and of Kormann et al. (2016).

Our proxy for catchment memory, designed based on the long-term deviation of cumulative sSSY, shows a positive relationship between the availability of sediment sources and event peak SSC. We observe more events with higher peak SSC when sediment resources are still abundant (Figure 7c). This is in line with our expectations, as the presence of abundant sediment sources creates favourable conditions for the occurrence of extreme SSC events. It should be noted, however, that no relationship was visible when we reset the catchment memory each winter, implying that sediment stores build up and empty over several years. In our case, deviations in sediment storage developed and were tracked throughout the time series (10-12 years).

The combination of greater sediment availability and sufficient forcing (e.g., high-intensity rainfall or snowmelt) results in larger observed peak SSC. The only exception are those events that are (partly) driven by glacial melt. These events also occur frequently during conditions in which more sediment than usual has already been transported prior to the event (Figure S12f-i in Supporting Information). One potential explanation for this is that events driven by glacial melt rely on a different sediment source compared to those driven by snowmelt and precipitation, namely sediments from the glacier and its forefields (Mancini et al., 2024). Consequently, the transportation of sediments during glacial melt is independent of the availability

of sediments in other areas within the catchment. However, this is inconsistent with the fact that this method makes use of the catchment specific annual cumulative sSSY regime, which already accounts for the different sediment sources within a catchment. Possibly, these events occurred during an exceptional period of glacier retreat or glacier motion that exceeded the annual average, as rapid glacier retreat and areas of recently deglaciated terrain reveal effective sediment sources (Moore et al., 2009; Swift et al., 2005).

4.3 Limitations and generalizability

The results presented are associated with uncertainties, which result from a combination of uncertainties inherited from the underlying data and methodology. One important data-related limitation is the uncertainty in the turbidity-SSC relationship. Despite the many efforts by the Swiss and Austrian hydrographic services in collecting bi-weekly manual SSC samples, it is difficult to reconstruct the relationship between turbidity and SSC reliably. The non-linear regression model attempts to represent the relation of SSC with turbidity, but the actual variability in the relationship between turbidity and SSC will likely be more stochastic as it is influenced by the varying characteristics of the sediments in suspension (particle size, shape, density, and color) (Gippel, 1995; Merten et al., 2014) and is also strongly dominated by mass wasting (Battista et al., 2022). Nevertheless, the turbidity-SSC relationship is currently the most applied and accepted method to derive high-resolution SSC time series described in the literature, and has been used by Costa et al. (2018a); Pellegrini et al. (2023); Stott and Mount (2007); Thollet et al. (2021), among others. Because of the uncertainty in the turbidity-SSC relationship, we removed a few implausible outliers and decided to aggregate the data from 10 and 15 minutes to mean hourly values. Before analysing the annual SSC regimes, we had to smooth the time series over a 30-day window to account for the relatively short time series. A further limitation of this study is the limited availability of SSC data, which has resulted in a relatively small sample size. At the same time, comprehensive large-sample studies are scarce. By analysing 38 rivers across the Alps, we believe that our analyses capture the most important processes and their variability in space and time.

Other uncertainties can be related to the methodology, e.g. the hierarchical clustering approach, the definition of extreme events, and the event classification scheme developed. For the clustering of the annual SSC regimes, we applied a hierarchical clustering algorithm. As each clustering method has its advantages and disadvantages, we performed a sensitivity analysis comparing the results of hierarchical clustering with the ones resulting from k-means clustering. This showed that the clusters identified are relatively stable, regardless of the choice of the clustering technique. However, a well-known disadvantage of clustering in general is that the selected indicators can strongly influence the final clusters. We deliberately selected indicators that were able to capture the shape of the SSC regime, rather than the variation in magnitude or the synchronicity with the discharge regime. This choice is reflected in the clusters identified, which differ mostly in terms of the number and timing of the main peaks.

For the detection of extreme SSC events, we applied a peak-over-threshold approach which is widely used (Skålevåg et al., 2024; Hamshaw et al., 2018; Haddadchi and Hicks, 2021; Blöthe and Hoffmann, 2022). At the same time, the definition of extremes necessarily entails some degree of subjectivity and arbitrary decision-making. Instead of using the 99th percentile threshold, a lower threshold could have been selected (for instance at the 90th percentile). This would have resulted in the

extraction of more but less extreme events. Furthermore, the methodology employed to define the start and end of an event is inherently subjective. The definition of the start of extreme SSC events is rather straightforward as it is characterised by a sudden and pronounced increase in SSC, that is easily detectable by a change in the slope. However, determining the end of the event was more challenging. We tested and compared three different methods within the framework of a sensitivity analysis, including the use of the slope, another fixed threshold, or the decrease of SSC relative to the SSC peak (Figure S5 in Supporting Information). The duration and the calculated sSSY of the event varied slightly depending on the selected method. However, the sensitivity analysis demonstrated that our primary results and conclusions remain unaffected by such changes in the definition (Table S3 in Supporting Information).

The classification scheme that we presented here is relatively straightforward to apply and therefore explainable. It requires only few inputs (hourly precipitation and daily snow- and glacial melt) and is based on the relatively well-understood processes of sediment transport, while more complex processes of sediment availability are ignored for simplicity. Our event classification relies on our input data and as the snow and glacial melt data are evaluated over the larger Alpine domain, they might be more uncertain in smaller catchments and on shorter time scales. However, general melt patterns are well-represented. Since our classification focuses on the dominant processes, it is less sensitive to smaller-scale uncertainty and increases our trust in our classification. We show that the method is applicable to catchments of different sizes and the absence of glaciers does not have a detrimental impact on the results. Given that the threshold for differentiating between dominant transport processes is set at 1/3, one would expect a considerable number of precipitation-snowmelt events in catchments without glacial melt, but with substantial snowmelt contributions. However, our analysis indicates that this is not a concern, as the number of precipitation-snowmelt events is relatively limited even in non-glaciated catchments. Our event classification differs from existing classification techniques, such as those proposed by Millares and Moñino (2020) and Skålevåg et al. (2024), which both rely extensively on the SSC-discharge relationship. In fact, the analysis of the annual SSC regimes has led us to conclude that discharge is a poor predictor of SSC in some catchments, thereby supporting the decision to select only hydro-climatic drivers for the classification scheme.

Our choice of methods and the use of a large sample of catchments contribute to the generalisability of our results. The clustering of SSC regimes and the event classification scheme have been designed to be transferable to other catchments and regions. Thus, this study does not only improve our understanding of the complex hydrological-sedimentary response in the studied catchments, but it also opens the door to further large-sample studies focusing on SSC. Finally, our results and conclusions might be generalizable to other mountain regions with similar characteristics, because the catchments considered in our dataset covered a large variety of catchment characteristics (mean catchment elevation from 590m to 2889m, glacier cover from 0% to 33%, fraction of precipitation falling as snow from 0 to 0.34).

4.4 Implications of findings and outlook

The importance of snow- and glacial melt for both seasonal and event SSC dynamics, suggests that climate change might affect sediment concentrations and fluxes in Alpine rivers in the future. There is evidence that glacier retreat results in a potential increase in suspended sediment concentrations and fluxes, and this effect can last for decades and centuries in small

alpine watersheds (Moore et al., 2009; Buter et al., 2022). However, a long-term decline in suspended sediments delivered from glacial sources is anticipated under future climate change scenarios since the area of glacier cover and glacier erosion will decrease and glacier forefields will stabilize (Moore et al., 2009; Mancini et al., 2024). Future projections of sediment export for two catchments in Ötztal suggest a decrease in sediment export already in the coming decades, and imply that 'peak sediment' has already passed (Schmidt et al., 2024). This is in line with findings by Freudiger et al. (2020) who concluded that glacier peak water has already been reached in most of the catchments in the Swiss Alps in the past decades and will be reached in all catchments during the first half of this century, independent of the emission scenario. In addition, also for non-glaciated catchments, such as the Illgraben valley, one of the most geologically unstable regions of Switzerland, studies suggest a future decline in sediment transport (Hirschberg et al., 2021). Although future climate conditions are expected to favour an increase in the sediment transport capacity in this valley, a reduction in sediment supply produced by frost weathering may limit debris-flow activity and actual sediment transport.

In addition to alterations in glacial coverage, future changes in snow seasonality, reduced snow accumulation and coverage are also expected to influence sediment availability in catchments and concentrations in rivers (Maruffi et al., 2022). When sediment sources are covered by snow they are protected from erosion and not connected to the river system, resulting in a reduction in SSC during winter (Schmidt et al., 2022). Consequently, shorter periods with snow and generally reduced snow cover will lead to longer periods with potentially increased connectivity of sediment sources to the river, which may lead to higher SSC. Nevertheless, we hypothesize that an extended period during which sediments can be transported may also cause a depletion of sediment sources, resulting in lower SSC later in the year.

Likewise, the impact of future precipitation on changes in sediment concentration remains incompletely understood, particularly in combination with sediment availability. Heavy and extreme precipitation events in the summer months will occur with greater frequency and intensity (Wood and Ludwig, 2020; Martel et al., 2020), and such occurrences have the potential to cause significant erosion and an elevated annual yield (Schmidt et al., 2024). However, as a consequence of dilution, high precipitation and high discharge do not necessarily result in the highest suspended sediment concentrations (Lana-Renault et al., 2007). While these alterations in the contribution of rain, snowmelt, and glacial melt will result in a shift in the timing of runoff and discharge seasonality, their impact on the SSC regime remains uncertain. Our observation-based insights into the relationship between melt processes and SSC suggest future changes in SSC behaviour. However, targeted modelling and field experiments are needed to better understand the whole process chain from weathering to erosion, sediment storage and sediment transport, and to make reliable projections of future SSC.

5 Conclusions

In this paper, we identified the main factors influencing the spatial and seasonal variability of the annual SSC regime and the occurrence of extreme SSC events in 38 catchments in the Alpine region. Our results demonstrate that the annual SSC regime and extreme SSC events in small mountain catchments are substantially influenced by snow and ice, in contrast to low-elevation and large catchments where liquid precipitation is more important. The presence of glaciers and the magnitude and timing of

snowmelt are important factors influencing the annual SSC regime and controlling the timing of peak SSC, while geology-
and soil-related catchment characteristics and the annual discharge regime appear to have a smaller influence. Furthermore, we
present a novel classification scheme to categorise extreme SSC events into nine different event types. Our analysis of 2,398
extreme SSC events indicates that rainfall is the primary driver of SSC extremes, accounting for 85 % of all events. This shows
that slightly different processes are important for controlling extreme events compared to annual SSC regimes. However, in
high-elevation and partly glaciated catchments, up to 35 % of the events are still attributable to snow- and glacial melt. Events
with compounding drivers, namely glacial melt and high-intensity rainfall, result in the highest sediment concentrations and
area-specific yields. Events driven by glacial melt have a specific yield of, on average, 52 t km^{-2}, which means that ten of these
short-term extreme events account for the transport of the total annual sediment yield of an average catchment. Moreover, a
considerable proportion of the extreme SSC events (24 % of the total) resulted in peak SSC values exceeding 5 g L^{-1}, which
can have detrimental effects on aquatic ecosystems. These findings highlight the importance and impact of such events on the
water quality in Alpine rivers and give an indication of soil loss due to water erosion.

Data availability. The shapefiles of all catchments, including static catchment characteristics, annual regime data and event data are available
through HydroShare according to the FAIR data sharing principles: van Hamel and Brunner (2025). Suspended sediment concentration in
Alpine rivers - annual regimes and extreme events, HydroShare, https://doi.org/10.4211/hs.8ec269a1e512434c9acb76b74025e8f7

Author contributions. AVH developed the general idea and conceptualized the study with MiB and PM. JJ provided the snowmelt and glacial
melt data that was used as input. AVH compiled the data and performed the analysis. The first draft of the paper, including all the figures,
was written by AVH with contributions from all co-authors. MiB, PM, and JJ revised and edited the document.

Competing interests. The authors declare that they have no conflict of interest and that MIB is an editor with HESS

Acknowledgements. The authors would like to thank the Swiss Federal Office for the Environment and the Austrian Hydrographic Service
for data provision.

References

Aires, U. R. V., Silva, D. D. d., Fernandes Filho, E. I., Rodrigues, L. N., Uliana, E. M., Amorim, R. S. S., Ribeiro, C. B. d. M., and Campos, J. A.: Machine learning-based modeling of surface sediment concentration in Doce river basin, Journal of Hydrology, 619, 129 320, https://doi.org/10.1016/j.jhydrol.2023.129320, 2023.

Asselman, N. E. M.: Fitting and interpretation of sediment rating curves, Journal of Hydrology, 234, 228–248, https://doi.org/10.1016/S0022-1694(00)00253-5, 2000.

Battista, G., Schlunegger, F., Burlando, P., and Molnar, P.: Sediment Supply Effects in Hydrology-Sediment Modeling of an Alpine Basin, Water Resources Research, 58, e2020WR029 408, https://doi.org/10.1029/2020WR029408, 2022.

Bilotta, G. S., Burnside, N. G., Cheek, L., Dunbar, M. J., Grove, M. K., Harrison, C., Joyce, C., Peacock, C., and Davy-Bowker, J.: Developing environment-specific water quality guidelines for suspended particulate matter, Water Research, 46, 2324–2332, https://doi.org/10.1016/j.watres.2012.01.055, 2012.

Blöschl, G., Nester, T., Komma, J., Parajka, J., and Perdigão, R. a. P.: The June 2013 flood in the Upper Danube Basin, and comparisons with the 2002, 1954 and 1899 floods, Hydrology and Earth System Sciences, 17, 5197–5212, https://doi.org/10.5194/hess-17-5197-2013, publisher: Copernicus GmbH, 2013.

Blöthe, J. H. and Hoffmann, T.: Spatio-temporal differences dominate suspended sediment dynamics in medium-sized catchments in central Germany, Geomorphology, 418, 108 462, https://doi.org/10.1016/j.geomorph.2022.108462, 2022.

Bogen, J.: The impact of climate change on glacial sediment delivery to rivers, IAHS Publ. 325, Christchurch, New Zealand, 2008.

Borrelli, P., Märker, M., Panagos, P., and Schütt, B.: Modeling soil erosion and river sediment yield for an intermountain drainage basin of the Central Apennines, Italy, CATENA, 114, 45–58, https://doi.org/10.1016/j.catena.2013.10.007, 2014.

Brighenti, S., Tolotti, M., Bruno, M. C., Engel, M., Wharton, G., Cerasino, L., Mair, V., and Bertoldi, W.: After the peak water: the increasing influence of rock glaciers on alpine river systems, Hydrological Processes, 33, 2804–2823, https://doi.org/10.1002/hyp.13533, 2019.

Buter, A., Heckmann, T., Filisetti, L., Savi, S., Mao, L., Gems, B., and Comiti, F.: Effects of catchment characteristics and hydro-meteorological scenarios on sediment connectivity in glacierised catchments, Geomorphology, 402, 108 128, https://doi.org/10.1016/j.geomorph.2022.108128, 2022.

Coffey, R., Paul, M. J., Stamp, J., Hamilton, A., and Johnson, T.: A Review of Water Quality Responses to Air Temperature and Precipitation Changes 2: Nutrients, Algal Blooms, Sediment, Pathogens, JAWRA Journal of the American Water Resources Association, 55, 844–868, https://doi.org/10.1111/1752-1688.12711, 2019.

Collins, A. L., Naden, P. S., Sear, D. A., Jones, J. I., Foster, I. D. L., and Morrow, K.: Sediment targets for informing river catchment management: international experience and prospects, Hydrological Processes, 25, 2112–2129, https://doi.org/10.1002/hyp.7965, 2011.

Copernicus: EU-DEM v1.1 — Copernicus Land Monitoring Service, https://doi.org/https://doi.org/10.5270/ESA-c5d3d65, 2013.

Costa, A., Anghileri, D., and Molnar, P.: A Process–Based Rating Curve to model suspended sediment concentration in Alpine environments, Hydrology and Earth System Sciences Discussions, pp. 1–23, https://doi.org/10.5194/hess-2017-419, publisher: Copernicus GmbH, 2017.

Costa, A., Anghileri, D., and Molnar, P.: Hydroclimatic control on suspended sediment dynamics of a regulated Alpine catchment: a conceptual approach, Hydrology and Earth System Sciences, 22, 3421–3434, https://doi.org/10.5194/hess-22-3421-2018, publisher: Copernicus GmbH, 2018a.

695   Costa, A., Molnar, P., Stutenbecker, L., Bakker, M., Silva, T. A., Schlunegger, F., Lane, S. N., Loizeau, J.-L., and Girardclos, S.: Temperature signal in suspended sediment export from an Alpine catchment, Hydrology and Earth System Sciences, 22, 509–528, https://doi.org/10.5194/hess-22-509-2018, publisher: Copernicus GmbH, 2018b.

Deng, J., Camenen, B., Legout, C., and Nord, G.: Estimation of fine sediment stocks in gravel bed rivers including the sand fraction, Sedimentology, 71, 152–172, https://doi.org/10.1111/sed.13132, 2024.

700   Doomen, A. M. C., Wijma, E., Zwolsman, J. J. G., and Middelkoop, H.: Predicting suspended sediment concentrations in the Meuse river using a supply-based rating curve, Hydrological Processes, 22, 1846–1856, https://doi.org/10.1002/hyp.6767, 2008.

Duan: Smearing Estimate: A Nonparametric Retransformation Method, Journal of the American Statistical Association, 78, 605–610, 1983.

Freudiger, D., Vis, M., and Seibert, J.: Quantifying the contributions to discharge of snow and glacier melt, Hydro-CH2018 project, Commissioned by the Federal Office for the Environment (FOEN), Bern, Switzerland, 2020.

705   Gabella, M., Speirs, P., Hamann, U., Germann, U., and Berne, A.: Measurement of Precipitation in the Alps Using Dual-Polarization C-Band Ground-Based Radars, the GPM Spaceborne Ku-Band Radar, and Rain Gauges, Remote Sensing, 9, 1147, https://doi.org/10.3390/rs9111147, 2017.

Gariano, S. L. and Guzzetti, F.: Landslides in a changing climate, Earth-Science Reviews, 162, 227–252, https://doi.org/10.1016/j.earscirev.2016.08.011, 2016.

710   Giovannini, L., Davolio, S., Zaramella, M., Zardi, D., and Borga, M.: Multi-model convection-resolving simulations of the October 2018 Vaia storm over Northeastern Italy, Atmospheric Research, 253, 105 455, https://doi.org/10.1016/j.atmosres.2021.105455, 2021.

Gippel, C. J.: Potential of turbidity monitoring for measuring the transport of suspended solids in streams, Hydrological Processes, 9, 83–97, https://doi.org/10.1002/hyp.3360090108, 1995.

Godt, J. W., Baum, R. L., and Lu, N.: Landsliding in partially saturated materials, Geophysical Research Letters, 36,
715   https://doi.org/10.1029/2008GL035996, 2009.

Grayson, R., Finlayson, B., Gippel, C., and Hart, B.: The Potential of Field Turbidity Measurements for the Computation of Total Phosphorus and Suspended Solids Loads, Journal of Environmental Management, 47, 257–267, https://doi.org/10.1006/jema.1996.0051, 1996.

Habersack, H., Haimann, M., Kerschbaumsteiner, W., and Lalk, P.: Schwebstoffe im Fliessgewässer – Leitfaden zur Erfassung des Schwebstofftransportes, Tech. rep., Federal Ministry of Agriculture, Forestry, Regions and Water Management, Vienna, 2017.

720   Haddadchi, A. and Hicks, M.: Understanding the effect of catchment characteristics on suspended sediment dynamics during flood events, Hydrological Processes, 34, 1558–1574, https://doi.org/10.1002/hyp.13682, 2020.

Haddadchi, A. and Hicks, M.: Interpreting event-based suspended sediment concentration and flow hysteresis patterns, Journal of Soils and Sediments, 21, 592–612, https://doi.org/10.1007/s11368-020-02777-y, 2021.

Haiden, T., Kann, A., Wittmann, C., Pistotnik, G., Bica, B., and Gruber, C.: The Integrated Nowcasting through Comprehensive Analysis
725   (INCA) System and Its Validation over the Eastern Alpine Region, https://doi.org/10.1175/2010WAF2222451.1, section: Weather and Forecasting, 2011.

Hamshaw, S. D., Dewoolkar, M. M., Schroth, A. W., Wemple, B. C., and Rizzo, D. M.: A New Machine-Learning Approach for Classifying Hysteresis in Suspended-Sediment Discharge Relationships Using High-Frequency Monitoring Data, Water Resources Research, 54, 4040–4058, https://doi.org/10.1029/2017WR022238, 2018.

730   Hartmann, J. and Moosdorf, N.: The new global lithological map database GLiM: A representation of rock properties at the Earth surface, Geochemistry, Geophysics, Geosystems, 13, https://doi.org/10.1029/2012GC004370, 2012.

Hinderer, M., Kastowski, M., Kamelger, A., Bartolini, C., and Schlunegger, F.: River loads and modern denudation of the Alps — A review, Earth-Science Reviews, 118, 11–44, https://doi.org/10.1016/j.earscirev.2013.01.001, 2013.

Hirschberg, J., Fatichi, S., Bennett, G. L., McArdell, B. W., Peleg, N., Lane, S. N., Schlunegger, F., and Molnar, P.: Climate Change Impacts on Sediment Yield and Debris-Flow Activity in an Alpine Catchment, Journal of Geophysical Research: Earth Surface, 126, e2020JF005 739, https://doi.org/10.1029/2020JF005739, publisher: John Wiley & Sons, Ltd, 2021.

Hoch, J. M., Sutanudjaja, E. H., Wanders, N., van Beek, R. L. P. H., and Bierkens, M. F. P.: Hyper-resolution PCR-GLOBWB: opportunities and challenges from refining model spatial resolution to 1 km over the European continent, Hydrology and Earth System Sciences, 27, 1383–1401, https://doi.org/10.5194/hess-27-1383-2023, publisher: Copernicus GmbH, 2023.

Horowitz, A. J.: An evaluation of sediment rating curves for estimating suspended sediment concentrations for subsequent flux calculations, Hydrological Processes, 17, 3387–3409, https://doi.org/10.1002/hyp.1299, 2003.

Höge, M., Kauzlaric, M., Siber, R., Schönenberger, U., Horton, P., Schwanbeck, J., Floriancic, M. G., Viviroli, D., Wilhelm, S., Sikorska-Senoner, A. E., Addor, N., Brunner, M., Pool, S., Zappa, M., and Fenicia, F.: CAMELS-CH: hydro-meteorological time series and landscape attributes for 331 catchments in hydrologic Switzerland, Earth System Science Data, 15, 5755–5784, https://doi.org/10.5194/essd-15-5755-2023, publisher: Copernicus GmbH, 2023.

Janzing, J., Wanders, N., van Tiel, M., van Jaarsveld, B., Karger, D. N., and Brunner, M. I.: Hyper-resolution large-scale hydrological modelling benefits from improved process representation in mountain regions, EGUsphere, pp. 1–46, https://doi.org/10.5194/egusphere-2024-3072, publisher: Copernicus GmbH, 2024.

Kemp, P., Sear, D., Collins, A., Naden, P., and Jones, I.: The impacts of fine sediment on riverine fish, Hydrological Processes, 25, 1800–1821, https://doi.org/10.1002/hyp.7940, 2011.

Klingler, C., Schulz, K., and Herrnegger, M.: LamaH-CE: LArge-SaMple DAta for Hydrology and Environmental Sciences for Central Europe, Earth System Science Data, 13, 4529–4565, https://doi.org/10.5194/essd-13-4529-2021, publisher: Copernicus GmbH, 2021.

Kormann, C., Bronstert, A., Francke, T., Recknagel, T., and Graeff, T.: Model-Based Attribution of High-Resolution Streamflow Trends in Two Alpine Basins of Western Austria, Hydrology, 3, 7, https://doi.org/10.3390/hydrology3010007, number: 1 Publisher: Multidisciplinary Digital Publishing Institute, 2016.

Lana-Renault, N., Regüés, D., Martí-Bono, C., Beguería, S., Latron, J., Nadal, E., Serrano, P., and García-Ruiz, J.: Temporal variability in the relationships between precipitation, discharge and suspended sediment concentration in a small Mediterranean mountain catchment, Hydrology Research, 38, 139–150, https://doi.org/10.2166/nh.2007.003, 2007.

Li, D., Overeem, I., Kettner, A. J., Zhou, Y., and Lu, X.: Air Temperature Regulates Erodible Landscape, Water, and Sediment Fluxes in the Permafrost-Dominated Catchment on the Tibetan Plateau, Water Resources Research, 57, e2020WR028 193, https://doi.org/10.1029/2020WR028193, 2021.

Li, D., Zhang, T., Walling, D. E., Lane, S., Bookhagen, B., Tian, S., Overeem, I., Syvitski, J., Kettner, A. J., Park, E., Koppes, M., Schmitt, R. J. P., Sun, W., Ni, J., and Ehlers, T. A.: The competing controls of glaciers, precipitation, and vegetation on high-mountain fluvial sediment yields, Science Advances, https://www.science.org/doi/10.1126/sciadv.ads6196, publisher: American Association for the Advancement of Science, 2024.

Li, T., Wang, S., Fu, B., and Feng, X.: Frequency analyses of peak discharge and suspended sediment concentration in the United States, Journal of Soils and Sediments, 20, 1157–1168, https://doi.org/10.1007/s11368-019-02463-8, 2020.

Mancini, D., Roncoroni, M., Dietze, M., Jenkin, M., Müller, T., Ouvry, B., Miesen, F., Pythoud, Q., Hofmann, M., Lardet, F., Nicholas, A. P., and Lane, S. N.: Rates of Evacuation of Bedload Sediment From an Alpine Glacier Control Proglacial Stream Morphodynamics, Journal of Geophysical Research: Earth Surface, 129, e2024JF007 727, https://doi.org/10.1029/2024JF007727, 2024.

Mano, V., Nemery, J., Belleudy, P., and Poirel, A.: Assessment of suspended sediment transport in four alpine watersheds (France): influence of the climatic regime, Hydrological Processes, 23, 777–792, https://doi.org/10.1002/hyp.7178, 2009.

Martel, J.-L., Mailhot, A., and Brissette, F.: Global and Regional Projected Changes in 100-yr Subdaily, Daily, and Multiday Precipitation Extremes Estimated from Three Large Ensembles of Climate Simulations, https://doi.org/10.1175/JCLI-D-18-0764.1, section: Journal of Climate, 2020.

Maruffi, L., Stucchi, L., Casale, F., and Bocchiola, D.: Soil erosion and sediment transport under climate change for Mera River, in Italian Alps of Valchiavenna, Science of The Total Environment, 806, 150 651, https://doi.org/10.1016/j.scitotenv.2021.150651, 2022.

Merten, G. H., Capel, P. D., and Minella, J. P. G.: Effects of suspended sediment concentration and grain size on three optical turbidity sensors, Journal of Soils and Sediments, 14, 1235–1241, https://doi.org/10.1007/s11368-013-0813-0, 2014.

Millares, A. and Moñino, A.: Hydro-meteorological drivers influencing suspended sediment transport and yield in a semi-arid mountainous basin, Earth Surface Processes and Landforms, 45, 3791–3807, https://doi.org/10.1002/esp.5001, 2020.

Mishra, A., Alnahit, A., and Campbell, B.: Impact of Land uses, Drought, Flood, Wildfire, and Cascading events on Water Quality and Microbial Communities: A Review and Analysis, Journal of Hydrology, https://doi.org/10.1016/j.jhydrol.2020.125707, 2020.

Misset, C., Recking, A., Legout, C., Poirel, A., Cazilhac, M., Esteves, M., and Bertrand, M.: An attempt to link suspended load hysteresis patterns and sediment sources configuration in alpine catchments, Journal of Hydrology, 576, 72–84, https://doi.org/10.1016/j.jhydrol.2019.06.039, 2019.

Mohamadi, M. A. and Kavian, A.: Effects of rainfall patterns on runoff and soil erosion in field plots, International Soil and Water Conservation Research, 3, 273–281, https://doi.org/10.1016/j.iswcr.2015.10.001, 2015.

Moore, R. D., Fleming, S. W., Menounos, B., Wheate, R., Fountain, A., Stahl, K., Holm, K., and Jakob, M.: Glacier change in western North America: influences on hydrology, geomorphic hazards and water quality, Hydrological Processes, 23, 42–61, https://doi.org/10.1002/hyp.7162, 2009.

Moosdorf, N., Cohen, S., and Von Hagke, C.: A global erodibility index to represent sediment production potential of different rock types, Applied Geography, 101, 36–44, https://doi.org/10.1016/j.apgeog.2018.10.010, 2018.

Muelchi, R., Rössler, O., Schwanbeck, J., Weingartner, R., and Martius, O.: River runoff in Switzerland in a changing climate – runoff regime changes and their time of emergence, Hydrology and Earth System Sciences, 25, 3071–3086, https://doi.org/10.5194/hess-25-3071-2021, publisher: Copernicus GmbH, 2021.

Newcombe, C. P. and Macdonald, D. D.: Effects of Suspended Sediments on Aquatic Ecosystems, North American Journal of Fisheries Management, 11, 72–82, https://doi.org/10.1577/1548-8675(1991)011<0072:EOSSOA>2.3.CO;2, 1991.

Nones, M. and Guo, Y.: Can sediments play a role in river flood risk mapping? Learning from selected European examples, Geoenvironmental Disasters, 10, 20, https://doi.org/10.1186/s40677-023-00250-9, 2023.

Panagos, P., Borrelli, P., Poesen, J., Ballabio, C., Lugato, E., Meusburger, K., Montanarella, L., and Alewell, C.: The new assessment of soil loss by water erosion in Europe, Environmental Science & Policy, 54, 438–447, https://doi.org/10.1016/j.envsci.2015.08.012, 2015.

Panagos, P., Matthews, F., Patault, E., De Michele, C., Quaranta, E., Bezak, N., Kaffas, K., Patro, E. R., Auel, C., Schleiss, A. J., Fendrich, A., Liakos, L., Van Eynde, E., Vieira, D., and Borrelli, P.: Understanding the cost of soil erosion: An assessment of the sediment removal costs

805   from the reservoirs of the European Union, Journal of Cleaner Production, 434, 140 183, https://doi.org/10.1016/j.jclepro.2023.140183, 2024.

Park, J. and Hunt, J. R.: Coupling fine particle and bedload transport in gravel-bedded streams, Journal of Hydrology, 552, 532–543, https://doi.org/10.1016/j.jhydrol.2017.07.023, 2017.

Parsons, A. J. and Stone, P. M.: Effects of intra-storm variations in rainfall intensity on interrill runoff and erosion, CATENA, 67, 68–78, 810   https://doi.org/10.1016/j.catena.2006.03.002, 2006.

Pellegrini, G., Mao, L., Rainato, R., and Picco, L.: Surprising suspended sediment dynamics of an alpine basin affected by a large infrequent disturbance, Journal of Hydrology, 617, 128 933, https://doi.org/10.1016/j.jhydrol.2022.128933, 2023.

Schmidt, L. K., Francke, T., Rottler, E., Blume, T., Schöber, J., and Bronstert, A.: Suspended sediment and discharge dynamics in a glaciated alpine environment: identifying crucial areas and time periods on several spatial and temporal scales in the Ötztal, Austria, Earth Surface 815   Dynamics, 10, 653–669, https://doi.org/10.5194/esurf-10-653-2022, publisher: Copernicus GmbH, 2022.

Schmidt, L. K., Francke, T., Grosse, P. M., Mayer, C., and Bronstert, A.: Reconstructing five decades of sediment export from two glacierized high-alpine catchments in Tyrol, Austria, using nonparametric regression, Hydrology and Earth System Sciences, 27, 1841–1863, https://doi.org/10.5194/hess-27-1841-2023, publisher: Copernicus GmbH, 2023.

Schmidt, L. K., Francke, T., Grosse, P. M., and Bronstert, A.: Projecting sediment export from two highly glacierized alpine catchments 820   under climate change: exploring non-parametric regression as an analysis tool, Hydrology and Earth System Sciences, 28, 139–161, https://doi.org/10.5194/hess-28-139-2024, publisher: Copernicus GmbH, 2024.

Shin, J. h., Grabowski, R. C., and Holman, I.: Indicators of suspended sediment transport dynamics in rivers, Hydrology Research, 54, 978–994, https://doi.org/10.2166/nh.2023.068, 2023.

Skålevåg, A., Korup, O., and Bronstert, A.: Inferring sediment-discharge event types in an alpine catchment from sub-daily time series, 825   Hydrology and Earth System Sciences Discussions, pp. 1–36, https://doi.org/10.5194/hess-2023-300, publisher: Copernicus GmbH, 2024.

Stein, L., Pianosi, F., and Woods, R.: Event-based classification for global study of river flood generating processes, Hydrological Processes, 34, 1514–1529, https://doi.org/10.1002/hyp.13678, _eprint: https://onlinelibrary.wiley.com/doi/pdf/10.1002/hyp.13678, 2020.

Steingruber, S. M., Bernasconi, S. M., and Valenti, G.: Climate Change-Induced Changes in the Chemistry of a High-Altitude Mountain Lake in the Central Alps, Aquatic Geochemistry, 27, 105–126, https://doi.org/10.1007/s10498-020-09388-6, 2021.

830   Stott, T. and Mount, N.: Alpine proglacial suspended sediment dynamics in warm and cool ablation seasons: Implications for global warming, Journal of Hydrology, 332, 259–270, https://doi.org/10.1016/j.jhydrol.2006.07.001, 2007.

Sutanudjaja, E. H., van Beek, R., Wanders, N., Wada, Y., Bosmans, J. H. C., Drost, N., van der Ent, R. J., de Graaf, I. E. M., Hoch, J. M., de Jong, K., Karssenberg, D., López López, P., Peßenteiner, S., Schmitz, O., Straatsma, M. W., Vannametee, E., Wisser, D., and Bierkens, M. F. P.: PCR-GLOBWB 2: a 5 arcmin global hydrological and water resources model, Geoscientific Model Development, 11, 835   2429–2453, https://doi.org/10.5194/gmd-11-2429-2018, publisher: Copernicus GmbH, 2018.

Sutari, C. A. T., Perk, M. V. d., and Middelkoop, H.: Spatial and temporal patterns of suspended sediment concentrations in the Rhine River, IOP Conference Series: Earth and Environmental Science, 451, 012 080, https://doi.org/10.1088/1755-1315/451/1/012080, publisher: IOP Publishing, 2020.

Swift, D. A., Nienow, P. W., and Hoey, T. B.: Basal sediment evacuation by subglacial meltwater: suspended sediment transport from Haut 840   Glacier d'Arolla, Switzerland, Earth Surface Processes and Landforms, 30, 867–883, https://doi.org/10.1002/esp.1197, 2005.

Thollet, F., Rousseau, C., Camenen, B., Boubkraoui, S., Branger, F., Lauters, F., and Némery, J.: Long term high frequency sediment observatory in an alpine catchment: The Arc-Isère rivers, France, Hydrological Processes, 35, e14 044, https://doi.org/10.1002/hyp.14044, _eprint: https://onlinelibrary.wiley.com/doi/pdf/10.1002/hyp.14044, 2021.

845 Turowski, J. M., Rickenmann, D., and Dadson, S. J.: The partitioning of the total sediment load of a river into suspended load and bedload: a review of empirical data, Sedimentology, 57, 1126–1146, https://doi.org/10.1111/j.1365-3091.2009.01140.x, 2010.

van Hamel, A. and Brunner, M. I.: Suspended sediment concentration in Alpine rivers - annual regimes and extreme events, https://doi.org/10.4211/hs.8ec269a1e512434c9acb76b74025e8f7, 2025.

Vanmaercke, M., Poesen, J., Verstraeten, G., de Vente, J., and Ocakoglu, F.: Sediment yield in Europe: Spatial patterns and scale dependency, Geomorphology, 130, 142–161, https://doi.org/10.1016/j.geomorph.2011.03.010, 2011.

850 Verrelle, A., Glinton, M., Bazile, E., Le Moigne, P., Randriamampianina, R., Ridal, M., Berggren, L., Undén, P., Schimanke, S., Mladek, R., and Soci, C.: CERRA-Land sub-daily regional reanalysis data for Europe from 1984 to present, https://doi.org/10.24381/CDS.A7F3CD0B, 2022.

Virtanen, P., Gommers, R., Oliphant, T. E., Haberland, M., Reddy, T., Cournapeau, D., Burovski, E., Peterson, P., Weckesser, W., Bright, J., van der Walt, S. J., Brett, M., Wilson, J., Millman, K. J., Mayorov, N., Nelson, A. R. J., Jones, E., Kern, R., Larson, E., Carey, C. J., Polat,

855 , Feng, Y., Moore, E. W., VanderPlas, J., Laxalde, D., Perktold, J., Cimrman, R., Henriksen, I., Quintero, E. A., Harris, C. R., Archibald, A. M., Ribeiro, A. H., Pedregosa, F., and van Mulbregt, P.: SciPy 1.0: fundamental algorithms for scientific computing in Python, Nature Methods, 17, 261–272, https://doi.org/10.1038/s41592-019-0686-2, publisher: Nature Publishing Group, 2020.

Vázquez-Tarrío, D., Ruiz-Villanueva, V., Garrote, J., Benito, G., Calle, M., Lucía, A., and Díez-Herrero, A.: Effects of sediment transport on flood hazards: Lessons learned and remaining challenges, Geomorphology, 446, 108 976, 860 https://doi.org/10.1016/j.geomorph.2023.108976, 2024.

Walling, D. E.: Assessing the accuracy of suspended sediment rating curves for a small basin, Water Resources Research, 13, 531–538, https://doi.org/10.1029/WR013i003p00531, 1977.

Ward Jr., J. H.: Hierarchical Grouping to Optimize an Objective Function, Journal of the American Statistical Association, 58, 236–244, https://doi.org/10.1080/01621459.1963.10500845, 1963.

865 Wolf, S., Stenger, D., Steudtner, F., Esser, V., Lehmkuhl, F., and Schüttrumpf, H.: Modeling anthropogenic affected sediment transport in a mid-sized European river catchment–extension of the sediment rating curve equation, Modeling Earth Systems and Environment, 9, 3815–3835, https://doi.org/10.1007/s40808-023-01703-8, 2023.

Wood, R. R. and Ludwig, R.: Analyzing Internal Variability and Forced Response of Subdaily and Daily Extreme Precipitation Over Europe, Geophysical Research Letters, 47, e2020GL089 300, https://doi.org/10.1029/2020GL089300, 2020.

870 Zaharescu, D. G., Hooda, P. S., Burghelea, C. I., Polyakov, V., and Palanca-Soler, A.: Climate change enhances the mobilisation of naturally occurring metals in high altitude environments, Science of The Total Environment, 560-561, 73–81, https://doi.org/10.1016/j.scitotenv.2016.04.002, 2016.

Zambon, N., Johannsen, L. L., Strauss, P., Dostal, T., Zumr, D., Cochrane, T. A., and Klik, A.: Splash erosion affected by initial soil moisture and surface conditions under simulated rainfall, CATENA, 196, 104 827, https://doi.org/10.1016/j.catena.2020.104827, 2021.

875 Zhang, T., Li, D., Kettner, A. J., Zhou, Y., and Lu, X.: Constraining Dynamic Sediment-Discharge Relationships in Cold Environments: The Sediment-Availability-Transport (SAT) Model, Water Resources Research, 57, e2021WR030 690, https://doi.org/10.1029/2021WR030690, _eprint: https://onlinelibrary.wiley.com/doi/pdf/10.1029/2021WR030690, 2021.

Zheng, H., Miao, C., Jiao, J., and Borthwick, A. G. L.: Complex relationships between water discharge and sediment concentration across the Loess Plateau, China, Journal of Hydrology, 596, 126 078, https://doi.org/10.1016/j.jhydrol.2021.126078, 2021.